

# Physiological Acoustics

The analysis of sound in the peripheral auditory system solves three important problems. First, sound energy impinging on the head must be captured and presented to the transduction apparatus in the ear as a suitable mechanical signal; second, this mechanical signal needs to be transduced into a neural representation that can be used by the brain; third, the resulting neural representation needs to be analyzed by central neurons to extract information useful to the animal. This chapter provides an overview of some aspects of the first two of these processes. The description is entirely focused on the mammalian auditory system, primarily on human hearing and on the hearing of a few commonly used laboratory animals (mainly rodents and carnivores). Useful summaries of non-mammalian hearing are available [12.1]. Because of the large size of the literature, review papers are referenced wherever possible.

<b>12.1 The External and Middle Ear</b> .....	429
12.1.1 External Ear .....	429
12.1.2 Middle Ear .....	432
<b>12.2 Cochlea</b> .....	434
12.2.1 Anatomy of the Cochlea .....	434
12.2.2 Basilar-Membrane Vibration and Frequency Analysis in the Cochlea .....	436
12.2.3 Representation of Sound in the Auditory Nerve .....	441
12.2.4 Hair Cells .....	443
<b>12.3 Auditory Nerve and Central Nervous System</b> .....	449
12.3.1 AN Responses to Complex Stimuli .....	449
12.3.2 Tasks of the Central Auditory System ....	451
<b>12.4 Summary</b> .....	452
<b>References</b> .....	453

## 12.1 The External and Middle Ear

The external and middle ears capture sound energy and couple it efficiently to the cochlea. The problem that must be solved here is that sound in air is not efficiently absorbed by fluid-filled structures such as the inner ear. Most sound energy is reflected from an interface between air and water, and terrestrial animals gain up to 30 dB in auditory sensitivity by virtue of their external and middle ears.

Comprehensive reviews of the external and middle ears are available [12.2, 3]. Figure 12.1 shows an anatomical picture of the ear (Fig. 12.1a) and a schematic showing the important signals in this part of the system (Fig. 12.1b). The external ear collects sound from the ambient field ( $p_F$ ) and conducts it to the eardrum where sound pressure fluctuations ( $p_T$ ) are converted to mechanical motion of the middle-ear bones, the malleus (with velocity  $v_M$ ), the incus, and the stapes; the velocity of the stapes ( $v_S$ ) is the input signal to the cochlea, producing a pressure  $p_V$  in the scala vestibuli. The following sections describe the properties of the transfer function from  $p_F$  to  $p_V$ .

### 12.1.1 External Ear

The acoustical properties of the external ear transform the sound pressure ( $p_F$ ) in the free field to the sound pressure at the eardrum ( $p_T$ ). Two main aspects of this transformation important for hearing are:

1. efficient capture of sound impinging on the head; and
2. the directional sensitivity of the external ear, which provides a cue for localization of sound sources.

Figures 12.2a and 12.2b show external-ear transfer functions for the human and cat ear. These are the dB ratio of the sound pressure near the eardrum  $p_T$  (see the caption) to the sound in free field ( $p_F$ ). The free-field sound  $p_F$  is the sound pressure that would exist at the approximate location of the eardrum if the subject were removed from the sound field completely. Thus the transformation from  $p_F$  to  $p_T$  contains all the effects of putting the subject in the sound field, including those due to refraction and reflection of sound from the

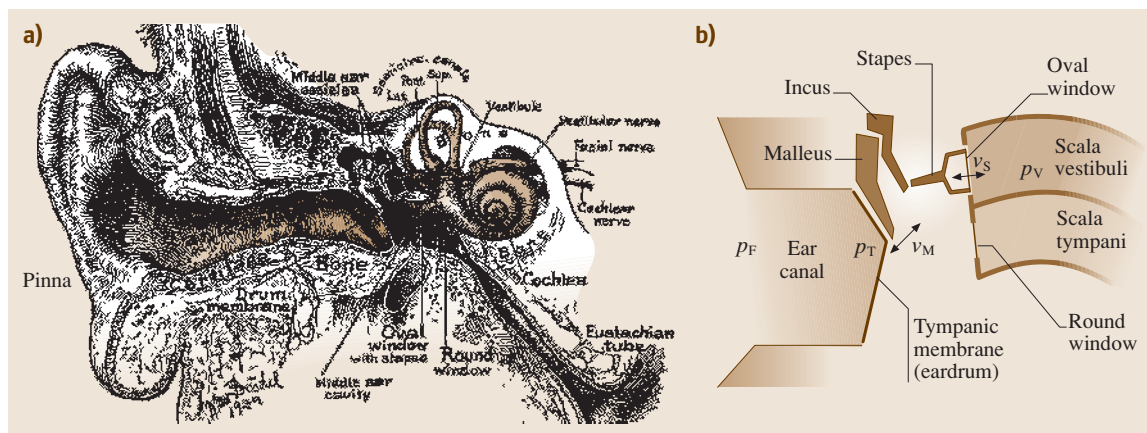


**Fig. 12.1** (a) Drawing of a cross section of the human ear, showing the pinna, the ear canal, eardrum (drum membrane), middle-ear bones (ossicles), and the labyrinth. The latter contains the vestibular organs of balance and the cochlea, or inner ear. (After [12.8]) (b) Schematic of the mammalian external and middle ears showing the signals referred to in the text. The middle-ear bones are the malleus, incus, and stapes. The stapes terminates on the cochlea, on a flexible membrane called the oval window. The velocity of the stapes ( $v_S$ ) is the input signal to the cochlea; it produces a pressure variation  $p_V$  in the fluids of the scala vestibuli, one of the chambers making up the cochlea. The structure of the cochlea and definitions of the scala vestibuli and scala tympani are shown in a later figure. The function of the external and middle ears is to capture the energy in the external sound field  $p_F$  and transfer it to stapes motion  $v_S$  or equivalently, sound pressure  $p_V$  in the scala vestibuli

surfaces of the body, the head, and the ear and the effects of propagation down the ear canal. In each case several transfer functions are shown. The dotted lines show  $p_T/p_F$  for sound originating directly in front of the subject [12.4, 5]; these curves are averaged across a number of ears. The solid lines show transfer functions measured in one ear from different locations in space [12.6, 7]. These have a fixed azimuth (i. e., position along the horizon, with  $0^\circ$  being directly in front of the subject) and vary in elevation (again  $0^\circ$  is directly in front) in the median plane. Elevations are given in the legends. External-ear transfer functions differ in detail from animal to animal. In particular, the large fluctuations at high frequencies, above 3 kHz in the human ear and 5 kHz in the cat ear, differ from subject to subject. These fluctuations are not seen in the averaged ears because they are substantially reduced by averaging across subjects, although some aspects of them remain [12.7]. However, the general features illustrated here are typical.

#### Capture of Sound Energy by the External Ear

Over most of the range of frequencies, the sound pressure is higher at the eardrum than in the free field in both the human (Fig. 12.2a) and the cat (Fig. 12.2b) subjects. The amplification results from resonances in the external ear canal and in the cavities of the pinna; the resonances

produce the broad peak between 2 and 5 kHz [12.2]. Although this seems to be an amplification of the sound field, the pressure gain is not by itself sufficient to specify fully the sound-collecting function of the external ear, because it is really the power collection that is important and sound power is the product of pressure and velocity. A useful summary measure of power collection is the effective cross-sectional area of the ear  $a_{ETM}$  [12.2, 9].  $a_{ETM}$  measures the ear's ability to collect sound from a diffuse pressure field incident on the head, in the sense that the sound power into the middle ear is equal to  $a_{ETM}$  multiplied by the power density in the sound field. If  $a_{ETM}$  is larger (smaller) than the anatomical area of the eardrum, for example, it means that the external ear is more (less) efficient at collecting sound than a simple eardrum-sized membrane located on the surface of the head.

Figure 12.2c shows calculations of the magnitude of  $a_{ETM}$  for the cat and human ear [12.2]. For comparison, the horizontal line shows the cross-sectional area of the external opening of the cat's pinna. Around 2–3 kHz,  $a_{ETM}$  equals the pinna area for the cat. The dotted line marked “ideal” is the maximum possible value of  $a_{ETM}$ , based on the power incident on a sphere in a diffuse field [12.2, 9]. At frequencies above 2 kHz, the cat ear is close to this maximum and the human ear is some-

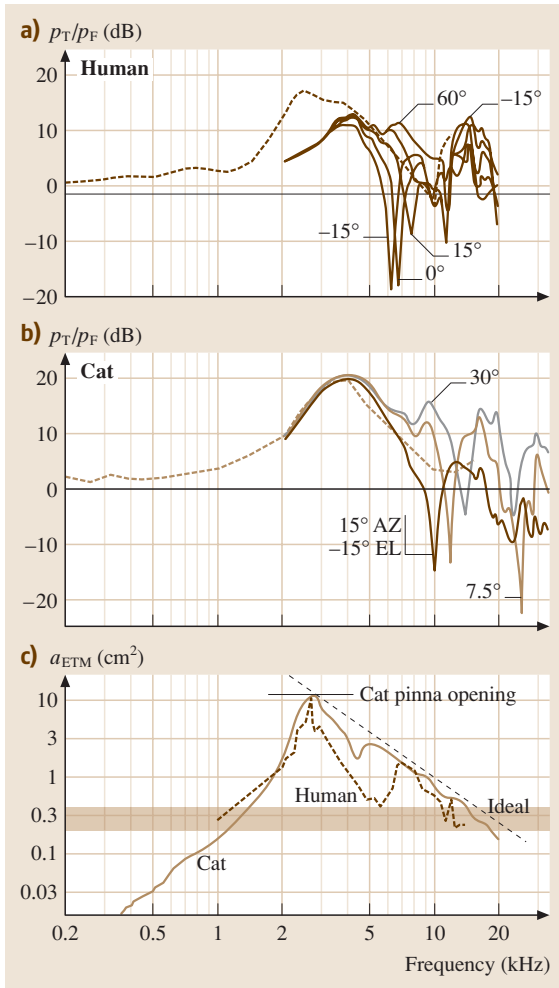


**Fig. 12.2a–c** Transformation of sound pressure by the external ear, considered as the ratio  $p_T/p_F$  for the human ear (a) and the cat ear (b).  $p_T$  is the pressure measured by a probe microphone in the ear canal, within 2 mm of the eardrum for all cases except the *solid curves* in (a), which show the pressure at the external end of the ear canal, with the ear canal blocked. The *dashed curves* are averaged across many ears, with the sound originating straight ahead, and the *solid curves* are data from one ear at various sound-source directions. The *numbers* next to the curves or in the legend identify the elevation of the sound source relative to the head. In both cases, the azimuth of the source is fixed. (c) Capture of sound energy by the external ear, considered as the effective cross-sectional area of the ear, mapped to the eardrum and plotted versus frequency. Curves for the cat and human ear are shown. The *shaded bar* shows the range of cross-sectional areas of the ear canal, for comparison. (Fig. 12.2a after [12.4, 7]; Fig. 12.2b after [12.5, 6]; Fig. 12.2c after [12.2])

comparing the values of  $a_{ETM}$  to the cross-sectional area of the ear canal, which is 0.2–0.4 cm<sup>2</sup> in cat, shown by the shaded bar [12.10].

### Directional Sensitivity

Directional sensitivity means that the transfer function of the external ear depends on the direction to the sound source. As a result, the spectra of broadband sounds (like noise) will be different, depending on the direction in space from which they originate. Listeners, both humans and non-human mammals, are sensitive to these differences and are able to extract sound localization information from them. For example, human observers use these so-called *spectral cues* to localize sounds in elevation and to disambiguate binaural difference cues, helping to distinguish sounds in front and behind the listener [12.11]. Cats depend on spectral cues to localize sounds in the frontal plane, both in azimuth and elevation [12.12].

The directional sensitivity of the external ear is generated by sound reflecting off the structures of the pinna. In humans the pinna is the cartilaginous structure attached to the external ear canal on the side of the head, and includes the cavities that lead to the entrance of the ear canal [12.13, 14]. In the cat, the pinna is a collection of similar cartilaginous shapes and cavities leading to the ear canal, most of which are located on the surface of the head at the ear canal opening. The external auricle, which forms the movable part of the cat's ear, serves as an additional sound collector and a way for the cat to change the directionality of its ear under vol-

what lower. At these frequencies, the external ear is collecting the sound power in a diffuse field nearly as efficiently as is possible. At lower frequencies, the efficiency drops rapidly; *Shaw* [12.9] attributes the drop off to three effects:

1. loss of pressure gain below the canal resonance
2. increase in the wavelength of sound compared to the size of the ear
3. increase in the impedance of the middle ear at low frequencies, decreasing the ability of the ear to absorb sound.

Figure 12.2c shows that the external ear can be considered as an acoustical horn that captures sound and couples it to the eardrum. A feeling for the effectiveness of the external ear's sound collection can be gotten by

untary control [12.15]. The nature of spectral cues in human and cat are shown in Figs. 12.2a,b. The most prominent spectral cue is the notch at mid frequencies (3–10 kHz in human and 7–20 kHz in cat). The notch is created as an interference pattern when sound propagates through the pinna. Essentially, there are multiple sound paths through the pinna due to reflections. These echoed sounds reach the ear canal after variable delays, depending on the path taken. At the ear canal, sounds can cancel at frequencies where the delays are approximately a half-cycle. The interference patterns so generated produce the notches shown in Fig. 12.2. The notches occur at relatively high frequencies, where the wavelength of sound is comparable to the lengths of the reflection paths in the pinna. In cats, the notch moves toward higher frequencies as the elevation (or the azimuth, not shown) increases [12.6, 16]. At higher frequencies, above 10 kHz in humans and 20 kHz in cat, there are additional complex changes in the transfer function of the external ear that are not easily summarized. Cats appear to be sensitive to spectral cues at all frequencies, but use the notch for localizing sounds and the higher-frequency characteristics for discriminating the locations of two sounds [12.17].

### 12.1.2 Middle Ear

The function of the middle ear is to transfer sound from the air to the fluids of the cochlea (e.g., from  $p_T$  to  $p_V$  in Fig. 12.1b). The process can be considered as an impedance transformation [12.18]. The specific acoustic impedance of a medium is the ratio of the sound pressure to the particle velocity of a plane wave propagating through the medium and is a property of the medium itself. When sound impinges on an interface between two media with different impedances, such as an air–water interface, energy is reflected from the boundary. In the case of air and water, the air is a low-impedance medium (low pressure, large velocity) and the water is high impedance medium (high pressure, low velocity). At the boundary, the pressure and velocity must be continuous, i. e. equal across the boundary. If the pressure is equal across the boundary, then the velocities must be different, larger in air than in water because of the differing impedances. A reflection occurs to allow both boundary conditions to be satisfied, i. e., the boundary conditions can only be satisfied by creating a third reflected wave at the boundary. The reflected wave, of course, takes energy away from the wave that propagates through the boundary. Maximum energy transfer across the boundary occurs when the impedance of the

source medium equals that of the second medium (no reflection). In the middle ear, the challenge is to transform the low impedance of air to the high impedance of the cochlea, so as to couple as much energy as possible into the cochlea.

The function of the middle ear as a impedance transformer is schematized in Fig. 12.3a which shows a drawing of the eardrum and the ossicles in approximately the anatomically correct position. In this model, the eardrum and oval window are assumed to act as pistons and the ossicles are assumed to act as a lever system, rotating approximately in the plane of the figure around the axis shown by the white dot in the head of the malleus [12.3]. The area of the eardrum ( $A_{TM}$ ) is larger than the area of the oval window ( $A_{OW}$ ), which increases the pressure by the ratio  $p_V/p_T = A_{TM}/A_{OW}$ . The difference in the lengths of the malleus and incus further increases the pressure by the lever ratio  $L_M/L_I$ , and decreases the velocity by the same amount. Thus the net pressure ratio is  $A_{TM}L_M/A_{OW}L_I$ . The area ratio amounts to a factor of 10–40 and the lever ratio is about 1.2–2.5 in mammalian ears [12.3]. For the cat, the pressure ratio should be about 36 dB. The impedance change is the ratio of the pressure and velocity ratios,  $A_{TM}/A_{OW}(L_M/L_I)^2$ , which is about 29 for the human ear [12.18]. This is less than the ideal value of 3500 for an air–water interface or 135 estimated for an air–cochlea interface, but is still a significant improvement (about 15 dB).

In reality, the motion of middle-ear components is more complex than is assumed in this model [12.2]. First, the eardrum does not displace as a simple piston; second the malleus and incus undergo a more complex motion than the one-dimensional rotation assumed in Fig. 12.3a; and third, there are losses in the motion of the ossicles that are not included in the model. Figure 12.3b shows a comparison of the actual pressure transformation in the middle ear of a cat, given as  $p_V/p_T$ . The dashed line is the prediction of the transformer model (36 dB). The cat ear gives a smaller pressure  $p_V$  than the transformer model for the reasons listed above, along with the fact that additional impedances in the middle ear must be considered when doing this calculation, such as the middle-ear cavity behind the eardrum, whose air is compressed and expanded as the eardrum moves [12.2]. Figure 12.3c shows the transfer function as it is usually displayed, as a transfer admittance from the eardrum pressure  $p_T$  to the velocity in the cochlea  $v_S$ .

The overall function of the external and middle ears in collecting sound from a diffuse field in the environment and delivering it to the cochlea is shown in

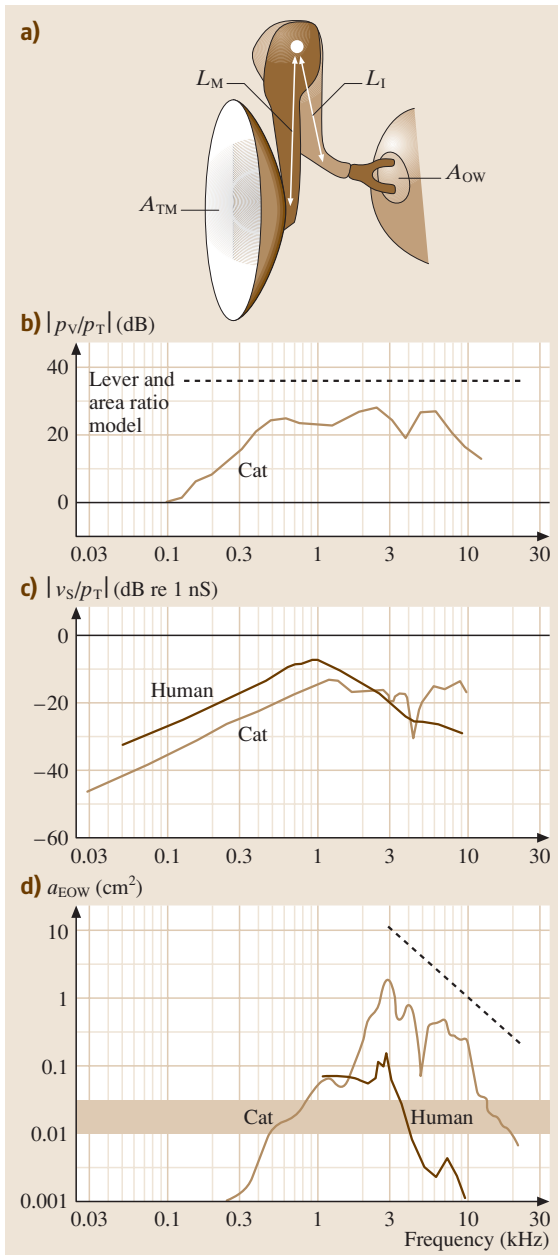


Fig. 12.3d [12.2]. This figure plots the effective area of the ear as a sound collector as in Fig. 12.2c, except now it refers to the sound power delivered to the oval win-

dow. Again, the dashed line shows the performance of an ideal spherical receiver and is the same line as in Fig. 12.2c. The effective area has a bandpass shape, as in Fig. 12.2c, with a maximum at 3 kHz. The sharp drop off in performance below 3 kHz was seen in the external ear analysis and occurs because energy is not absorbed at the eardrum at low frequencies. At higher frequencies the effective area tracks the ideal receiver, but is about 10–15 dB smaller than the performance at the eardrum, which approximates the ideal for the cat. This decrease reflects the losses in the middle ear discussed above. Although the external and middle ear do not approach ideal performance, they do serve to couple sound into the cochlea. As a comparison to the effective area in Fig. 12.3d, the cross-sectional area of the oval window is about 0.01–0.03 cm<sup>2</sup> in the cat and human (shaded bar). Thus the effective area is larger than the area of the oval window over the mid frequencies. Moreover, if there were no middle ear, the collecting cross section of the oval window would be smaller by about 15–30 dB because of the impedance mismatch between the air and cochlear fluids [12.19].

dow. Again, the dashed line shows the performance of an ideal spherical receiver and is the same line as in Fig. 12.2c. The effective area has a bandpass shape, as in Fig. 12.2c, with a maximum at 3 kHz. The sharp drop off in performance below 3 kHz was seen in the external ear analysis and occurs because energy is not absorbed at the eardrum at low frequencies. At higher frequencies the effective area tracks the ideal receiver, but is about 10–15 dB smaller than the performance at the eardrum, which approximates the ideal for the cat. This decrease reflects the losses in the middle ear discussed above. Although the external and middle ear do not approach ideal performance, they do serve to couple sound into the cochlea. As a comparison to the effective area in Fig. 12.3d, the cross-sectional area of the oval window is about 0.01–0.03 cm<sup>2</sup> in the cat and human (shaded bar). Thus the effective area is larger than the area of the oval window over the mid frequencies. Moreover, if there were no middle ear, the collecting cross section of the oval window would be smaller by about 15–30 dB because of the impedance mismatch between the air and cochlear fluids [12.19].

## 12.2 Cochlea

The cochlea contains the ear's transduction apparatus, by which sound energy is converted into electrical activity in nerve cells. The conversion occurs in transduction cells, called inner hair cells, and is transferred to neurons in the auditory nerve (AN) that connect to the brain. However the function of the cochlea is more than a transducer. The cochlea also does a frequency analysis, in which a complex sound such as speech or music is separated into its component frequencies, a process not unlike a Fourier or wavelet transform. Auditory perception is largely based on the frequency content of sounds; such features as the identity of sounds (which speech sound?), their pitches (which musical note?), and the extent to which they interact in the ear (e.g., to make it hard to hear one sound because of the presence of another) are determined by the mixture of frequencies making them up (Chap. 13).

In this section, the steps in the transduction process in the inner ear or cochlea are described. The problems solved in this process include frequency analysis, mentioned above, but also regulating the sensitivity of process. Transduction must be very sensitive at low sound levels, so that sounds can be detected near the limit imposed by Brownian motion of the components of the cochlea [12.20]. At the same time, the cochlea must function over the wide dynamic range of sound intensities (up to 100 dB or more) that we encounter in the world. Responses to this wide dynamic range must be maintained in neurons with much more limited dynamic ranges, 20–40 dB [12.21]. In part this is accomplished by compressing the sound in the transduction process, so that acoustic sound intensities varying over a range of 60–100 dB are mapped into neural excitation over a much more limited dynamic range. Thus cochlear sensitivity must be high at low sound levels to allow soft sounds to be heard and must be reduced at high sound levels to maintain responsiveness without saturation. Both frequency tuning and dynamic-range adjustment depend on the same cochlear element, the second set of transducer cells called outer hair cells. Whereas inner hair cells convey the representation of sound to the AN, the outer hair cells participate in cochlear transduction itself, making the cochlea more sensitive, increasing its frequency selectivity, and compressing its dynamic range. These processes are described in more detail below.

The remainder of this chapter assumes some knowledge of neural excitation and synaptic transmission. These subjects are too extensive to review here, but

can be quickly grasped from an introductory text on neurophysiology or neuroscience.

### 12.2.1 Anatomy of the Cochlea

The inner ear consists of the cochlea and the AN. The cochlea contains the transduction apparatus; it is a coiled structure, as shown in Fig. 12.1a. A cross-sectional view of a cochlea is shown in Fig. 12.4a. This figure is a low-resolution sketch that is provided to show the locations of the major parts of the structure. The section is cut through the center of the cochlear coil and shows approximately 3.5 turns of the coil. The cochlea actually consists of three fluid-filled chambers (or *scalae*) that coil together. A cross section of one turn of the spiral showing the three chambers is in Fig. 12.4b. The *scala tympani* (ST) and *scala media* (SM) are separated by the basilar membrane, a complex structure consisting of connective tissue and several layers of epithelial cells. The *scala vestibuli* (SV) is separated from the SM by Reissner's membrane, a thin epithelial sheet consisting of two cell layers. Reissner's membrane is not important mechanically in the cochlea and is usually ignored when discussing cochlear function. In the following, the mechanical properties of the basilar membrane are discussed without reference to the Reissner's membrane and it is usual to speak of the basilar membrane as if it separated the SV and ST.

What Reissner's membrane does do is to separate the fluids of the SV from the SM. The fluids in the SV and ST are typical of the fluids filling extracellular spaces in the body; this fluid, called *perilymph* is basically a dilute NaCl solution, with a variety of other constituents but with low  $K^+$  concentration. In contrast, the fluid in SM, called *endolymph*, has a high  $K^+$  concentration with low  $Na^+$  and  $Ca^{2+}$  concentrations. Such a solution is rare in extracellular spaces, but is commonly found bathing the apical surfaces of hair cells in sensory organs from insects to mammals, suggesting that the high potassium concentration is important for hair-cell function. The endolymph is generated in the *stria vascularis*, a specialized epithelium in the lateral wall of the SM by a complex multicellular active-transport system [12.22].

Mounted on the basilar membrane is the organ of Corti, which contains the actual cochlear transduction apparatus, shown in more detail in Fig. 12.4c. The organ of Corti consists of supporting cells and hair cells. There are two types of hair cells, called inner (IHC) and outer

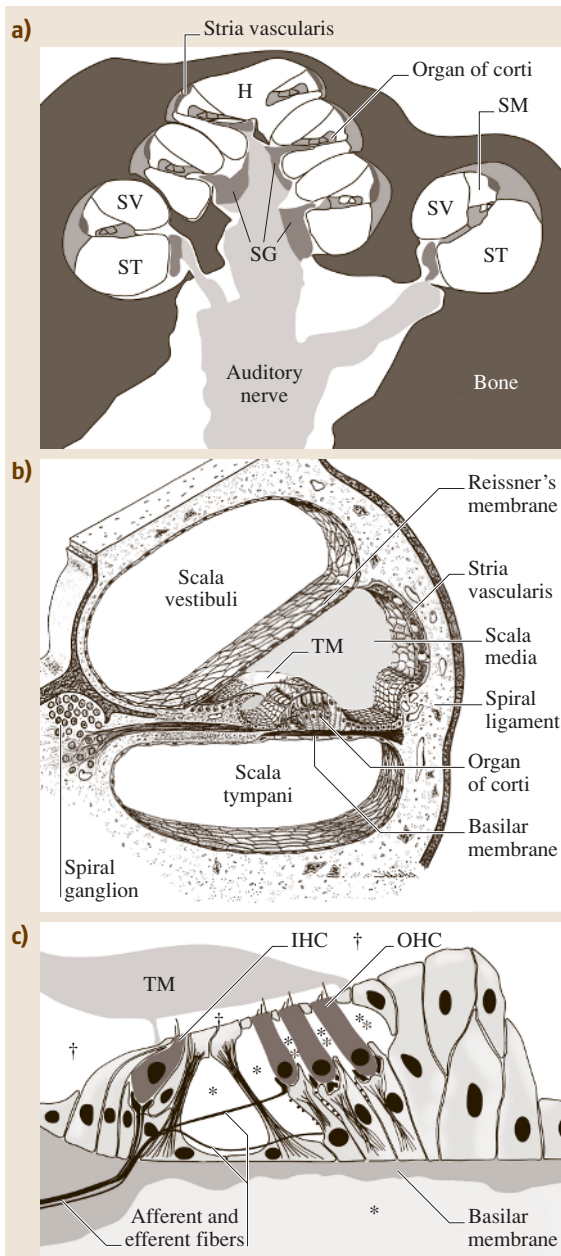


**Fig. 12.4** (a) Sketch of a cross section of the cochlea, cut through the center of the coil. The cochlear spirals are cut in cross section, shown at higher resolution in (b). The cochlea consists of three fluid-filled chambers that spiral together: **ST** – scala tympani, **SV** – scala vestibuli, and **SM** – scala media. **H** is the helicotrema, a connection between the **SV** and **ST** at the apex of the cochlea. The cochlear transducer has three essential functional parts:

1. the basilar membrane which separates the **SM** and **ST**;
2. the organ of Corti, which contains the hair cells, and
3. the stria vascularis which secretes the fluid in the **SM** and provides an energy source to the transducer.

The **AN** fibers have their cell bodies in the spiral ganglion (**SG**); their axons project to the brain in the **AN**. (b) Cross section of the cochlear spiral showing the three scalae. The scalae are fluid-filled; the **SV** and **ST** contain perilymph. The **SM** contains endolymph. (c) Schematic drawing of the organ of Corti showing the inner (**IHC**) and outer hair cells (**OHC**) and several kinds of supporting cells. The spaces containing perilymph are marked with *asterisks* and the spaces containing endolymph with *daggers* (†). **TM** is the tectorial membrane, which lies on the organ of Corti and is important in stimulating the hair cells. Nerve fibers enter the organ from the **SG** (off to the left). Both afferent and efferent fibers are present. Afferents are the **SG** neurons that are connected synaptically to hair cells, mainly **IHCs**, and carry information to the brain. Efferents are the axons of neurons located in the brain which connect to **OHCs** and to the afferents under the **IHCs** (Fig. 12.5). (After [12.23])

The arrangement of the nerve fibers in the cochlea is reviewed in detail by *Ryugo* [12.24] and by *Warr* [12.25] and is summarized in Fig. 12.5. Both afferent and efferent fibers are present. The afferents are the neurons mentioned above with their cell bodies in the **SG** which carry information from the hair cells to the brain. The efferents are the axons of neurons in the brain that terminate in the cochlea and allow central control of cochlear transduction.

Considering the afferents firsts, there are two groups of **SG** neurons, called type I and type II. Type I neurons make up about 90–95% the population; their distal processes travel directly to the **IHC** in the organ of Corti. Each type I neuron innervates one **IHC**, and each hair cell receives a number of type I fibers; the exact number varies with species and location in the cochlea, but is typically 10–20. The connection between the **IHC** and type I hair cells is a standard chemical synapse, by which the hair cell excites the **AN** fiber. Type I **AN** fibers project into the core areas of the cochlear nucleus, the

(**OHC**), because of their positions. The **AN** fibers and their cell bodies in the spiral ganglion (**SG** in Fig. 12.4a) occupy the center of the cochlear coil. Spiral ganglion cells have two processes: a distal process that invades the organ of Corti and innervates one or more hair cells, usually an **IHC**, and a central process that travels in the **AN** to the brain.

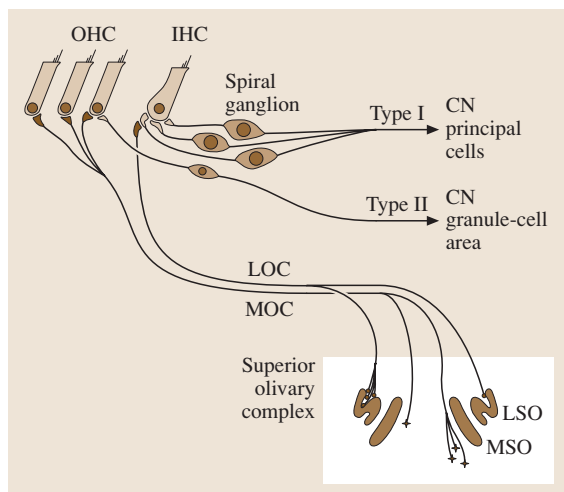


**Fig. 12.5** A schematic of the wiring diagram of the mammalian cochlea. The hair cells are on the left. Afferent terminals on hair cells, those in which the hair cell excites an AN fiber, are shown *lightly shaded*; efferent terminals, in which an axon from a cell body in the central nervous system contacts a hair cell or another terminal in the organ of Corti, are shown *heavily shaded*. All the synapses in the cochlea are chemical. Inner hair cells (IHC) are contacted by the distal processes of AN fibers. These fibers have bipolar cell bodies in the spiral ganglion; their axons are myelinated and travel centrally (type I fibers) to innervate principal neurons in the cochlear nucleus (CN). Outer hair cells (OHC) are innervated by a small population of type II spiral ganglion cells whose axons terminate in granule cell regions in the CN. The efferent fibers to the cochlea are called olivocochlear neurons; they originate in the superior olivary complex (SOC, box at lower right), another part of the central auditory system. There are two kinds of efferents: the medial olivocochlear system (MOC), originates near the medial nucleus of the SOC and innervates OHCs. The lateral olivocochlear system (LOC) originates near the lateral nucleus of the SOC and innervates afferent terminals of type I afferent fibers under the IHCs. The MOC and LOC contain fibers from both sides of the brain, although most LOC fibers are ipsilateral and most MOC fibers are contralateral, as drawn. The exact ratios vary with the animal

first auditory structure in the brain; the type I fibers plus the neurons in the core of the cochlear nucleus make up the main pathway for auditory information entering the brain.

The remaining 5–10% of the spiral ganglion neurons, type II, innervate OHCs. The fibers cross the

fluid spaces between the IHC and the OHC (shown by the asterisks in Fig. 12.4c) and spiral along the basilar membrane beneath the OHCs toward the base of the cochlea (toward the stapes, not shown) innervating a few OHCs along the way. Although the type II fibers are like type I fibers in that they connect hair cells (in this case OHC) to the cochlear nucleus, there are some important differences. The axons of type II SG neurons are unmyelinated, unlike the type I fibers; their central processes terminate in the granule-cell areas of the cochlear nucleus, where they contact interneurons, meaning neurons that participate in the internal circuitry of the nucleus but do not contribute their axons to the outputs of the nucleus. Finally, type II fibers do not seem to respond to sound [12.26–28], even though they do propagate action potentials [12.29, 30]. It is clear that the type I fibers are the main afferent auditory pathway, but the role of the type II fibers is unknown. In the remainder of this chapter, the term *AN fiber* refers to type I fibers only.

The efferent neurons have their cell bodies in an auditory structure in the brain called the superior olivary complex; for this reason, they are called the olivocochlear bundle (OCB). The anatomy and function of the OCB efferents are reviewed by Warr [12.25] and by Guinan [12.31]. Anatomically, there are two groups of OCB neurons. So-called lateral efferents (LOC) travel mainly to the ipsilateral cochlea and make synapses on the dendrites of type I afferents under the IHC. Thus they affect the afferent pathway directly. The second group, medial efferents (MOC), travel to both the ipsilateral and contralateral ears and make synapses on the OHCs. Their effect on the afferent pathway is thus indirect, in that they act through the OHC's effects on the transduction process in the cochlea.

### 12.2.2 Basilar-Membrane Vibration and Frequency Analysis in the Cochlea

An overview of the steps in cochlear transduction is shown in Fig. 12.6a. The sound pressure at the eardrum ( $p_T$ ) is transduced into motion of the middle-ear ossicles, ultimately resulting in the stapes velocity ( $v_S$ ), which couples sound energy into the SV. The transformations in this part of the system have mainly to do with acoustical mechanics and were described in the first section above. The stapes motion produces a sound pressure signal in the cochlea that results in vibration of the basilar membrane, which is the topic of this section. The vibration results in stimulation of hair cells, through opening and closing of transduction channels



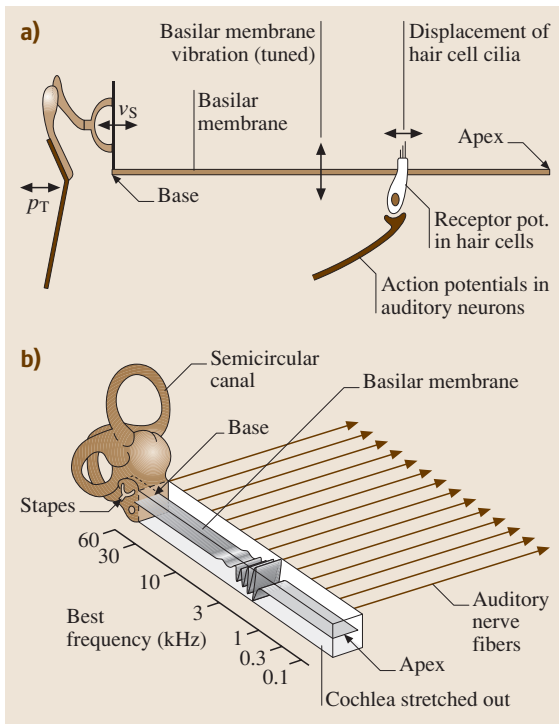


**Fig. 12.6** (a) Summary of the steps in direct cochlear transduction. (b) Schematic diagram showing the basilar membrane in an unrolled cochlea and the nature of cochlear frequency analysis. A snapshot of basilar-membrane displacement (greatly magnified) by a tone with frequency near 3 kHz is shown. The frequency *left scale* shows the location of the maximum membrane displacement at various frequencies for a cat cochlea. For a human cochlea, the frequency scale runs from about 20 Hz to 15 kHz. The array of AN fibers is shown by the *parallel lines on the right*. Each fiber innervates a hair cell at one place on the basilar membrane, so the fiber's sensitivity is maximal at the frequency corresponding to that place, as shown by the *left scale*. In other words, the separation of frequencies done by the basilar membrane is preserved in the AN fiber array. (After [12.32] with permission)

built into the cilia that protrude from the top of the hair cell, described in a later section. The hair cells are synaptically coupled to AN fibers, so that basilar-membrane vibration is eventually coupled to activation of the nerve.

A key aspect of cochlear function is frequency analysis. The nature of cochlear frequency analysis is illustrated in Fig. 12.6b, which shows the cochlea uncoiled, with the basilar membrane stretching from the

base, the end near the stapes, to the apex (the helicotrema). As described above, the basilar membrane lies between (separates) the ST and the SM/SV. The sound entering the cochlea through the vibration of the stapes is coupled into the fluids of the SV and SM at the base, above the basilar membrane in Fig. 12.6. The sound energy produces a pressure difference between the SV/SM and the ST, which causes vertical displacement of the basilar membrane. The displacement is tuned, in that the motion produced by sound of a particular frequency is maximum at a particular place along the cochlea. The resulting place map is shown by the frequency scale on the left in Fig. 12.6. Basilar-membrane displacement was first observed and described by von Békésy [12.33]; more recent data are reviewed by Robles and Ruggero [12.34].

### Basilar-Membrane Motion

The displacement of any single point on the basilar membrane is an oscillation vertically (perpendicular to the surface of the membrane); the relative phase (or timing) of the oscillations of adjacent points is such that the overall displacement looks like a traveling wave, frequently described as similar to the waves propagating away from an object dropped into a pool of water. Essentially, the motion of the basilar membrane is delayed in time as the observation point moves from base to apex. Figure 12.7a shows an estimate of the cochlear traveling wave on the guinea-pig basilar membrane, based on electrical potentials recorded across the membrane [12.35]. The horizontal dimension in this figure is distance along the basilar membrane, with the base at left and the apex at right. The vertical dimension is the estimate of displacement, shown at a greatly expanded scale. The oscillations marked “2 kHz” show membrane deflections in response to a 2 kHz tone at five successive instants in time (labeled 1–5). The wave appears to travel rightward, from the base toward the apex; as it does so, its amplitude changes. When the stimulus is a tone, the displacement envelope (i. e., the maximum amplitude of the displacement at each point along the basilar membrane) has a single peak at a location that depends on the tone frequency (approximately at point 2 in this case). In Fig. 12.7a, displacement envelopes are shown by dashed lines for 0.5 kHz and 0.15 kHz tones; these envelopes peak at more apical locations, compared to 2 kHz. The locations of the envelope peaks are given by the cochlear frequency map for the cat cochlea, shown by the scale running along the basilar membrane in Fig. 12.6b. Notice that the scale is logarithmic: the position along the basilar membrane corresponds more

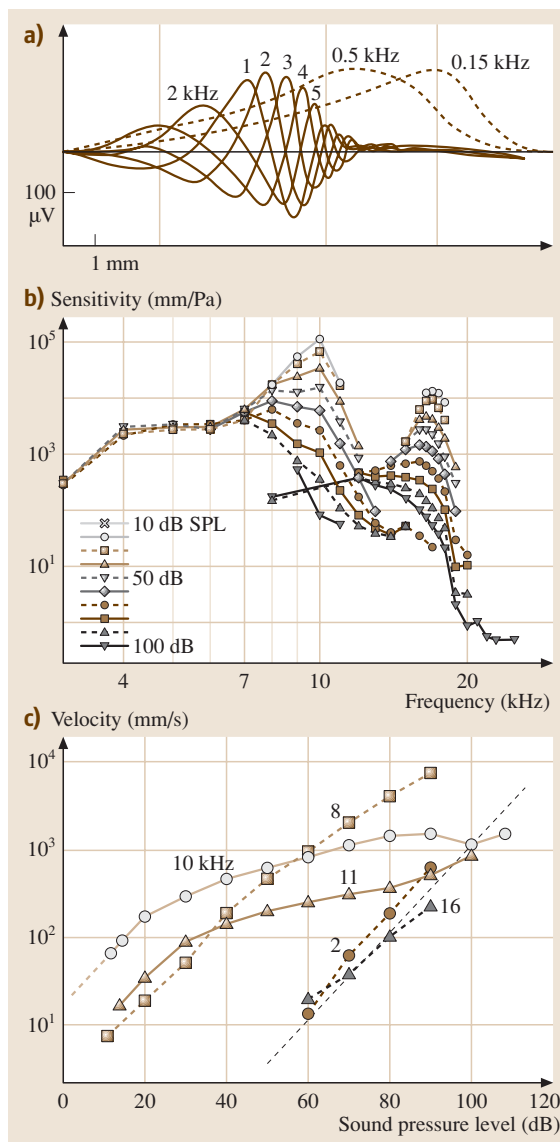


**Fig. 12.7** (a) An estimate of the instantaneous displacement of the basilar membrane in the guinea-pig cochlea for a 2 kHz tone (*solid lines*) and estimates of the envelope of the displacement for two lower-frequency tones (*dashed lines*). Distance along the basilar membrane runs from left (*base*) to right (*apex*) and the displacement of the membrane is plotted vertically. The estimates were obtained by measuring the cochlear microphonic at three sites, indicated by the three vertical lines, and then interpolating or extrapolating to other locations using an informal method [12.35]; this method can be expected to produce only qualitatively correct results. The 2 kHz estimates are shown at 0.1 ms intervals. Waveforms at successive times are identified with the numbers “1” through “5”. The *dashed curves* were drawn through the maximum displacements of similar data for 0.5 and 0.15 kHz tones, which were scaled to have the same maximum displacement as the 2 kHz data. The cochlear microphonic is produced by hair cells, mainly OHCs, and is roughly proportional to basilar-membrane displacement. The ordinate scale has been left as microvolts of cochlear microphonic. The scale markers at lower left show distance from the origin. (b) Measurements of the gain of the basilar membrane (root mean square displacement divided by pressure at the eardrum) for two data sets. In each case, basilar-membrane displacement at one place was measured with an interferometer. Both frequency (abscissa) and sound level (symbols) were varied. The curves peaking near 9–10 kHz are from the chinchilla cochlea [12.36] and the curves peaking near 20 kHz are from the guinea pig cochlea [12.37] (After [12.34]). (c) Basilar-membrane input–output curves, showing the velocity of membrane displacement (*ordinate*) versus sound intensity (*abscissa*), at various frequencies, marked on the plots (kHz). The *dashed line at right* shows the linear growth of basilar-membrane motion (velocity proportional to sound pressure). The curve for 10 kHz is extrapolated to low sound levels (*dashed line at left*) under the assumption of linear growth at low sound levels (Fig. 12.7a after [12.35], Fig. 12.7b after [12.34], and Fig. 12.7c after [12.36])

closely to log than to linear frequency. The logarithmic frequency organization corresponds to a number of phenomena in the perception of sound, such as the fact that musical notes are spaced logarithmically in frequency.

The basilar-membrane responses in Fig. 12.7a illustrate the property of tuning, in that the displacement in response to a tone is confined to a region of the membrane centered on a place of maximal displacement. Tuning can be further understood by plotting basilar-membrane displacement as in Fig. 12.7b. This

plot shows the displacement plotted against frequency at a fixed location, thus providing a direct measure of the frequency sensitivity of a place on the membrane. Data are shown at two locations from separate experiments (in different species). The ordinate actually shows basilar-membrane *gain*, defined as membrane displacement divided by sound pressure at the eardrum. At low sound levels (20 dB, plotted with empty circles), the gain peaks at a particular best frequency (BF) and decreases at adjacent frequencies. If such measurements could be repeated at multiple locations along the basilar membrane

(which is difficult because of the restricted anatomical access to the basilar membrane), these gain functions would move toward higher frequencies at more basal locations in the cochlea, as predicted by the displacement functions in Fig. 12.7a.

Notice that the gain and tuning of the basilar-membrane response near the BF varies with sound level. At low sound levels (20 dB in Fig. 12.7b), gain is high and the tuning is sharp (i. e. the width of the gain functions is small), giving a clear BF; at high sound levels (100 dB), the gain is substantially reduced, especially in the vicinity of the low-sound-level BF, and the frequency at which the gain is maximum moves to a lower frequency, often about a half-octave lower. The tuning also becomes much broader.

### Basilar Membrane and Compression

The fact that basilar-membrane gain changes with sound level was first described by *Rhode* [12.38]; this finding revolutionized our understanding of the auditory system, most importantly by introducing the idea of an active cochlea, meaning one in which the acoustic energy entering through the middle ear is amplified by an internal energy-utilizing process to produce cochlear responses [12.39–44]. The existence of amplification has been demonstrated by calculations of energy flow in the cochlea. However, a simpler evidence for cochlear amplification is the change in cochlear gain functions with death. The dependence of gain on sound level seen in Fig. 12.7b occurs only in the live, intact cochlea; after death, the cochlear gain functions resemble those at the highest sound levels in living animals (e.g. at 100 dB in Fig. 12.7b). Most important, the post-mortem gain functions are linear, meaning that the gain is constant, regardless of stimulus intensity, at all frequencies. In the live cochlea, as shown in Fig. 12.7b, the gain functions are linear only at low frequencies (below 6 kHz or 12 kHz for the two sets of data shown). Presumably, the post-mortem gain functions are the result of passive basilar-membrane mechanics, i. e., the result of the mechanical properties of the cochlea without any energy sources. The difference between the gain at the highest sound levels in Fig. 12.7b and those at low sound levels thus reflects an amplification process, often called the cochlear amplifier.

Additional evidence for a cochlear amplifier comes from the study of otoacoustic emissions, OAE [12.45, 46]. OAEs are sounds produced in the cochlea that can be measured at the eardrum, after propagating in the backwards direction through the middle ear. OAEs can be produced by reflection of the cochlear traveling wave

from irregularities in the cochlea [12.47, 48] or from nonlinear distortion in elements of the cochlea [12.49]. In either case amplification of the sound is necessary to explain the characteristics of the emitted sound [12.46], but see also [12.50]. There are several different kinds of OAEs, varying in the mode of production. Most relevant for the present discussion are the spontaneous emissions, sounds that are present in the ear canal without any external sound source. Such sounds necessitate an acoustic energy source in the cochlea, of the type postulated for the cochlear amplifier.

A variety of evidence suggests that cochlear amplification depends on the OHCs. When these cells are destroyed, as by an ototoxic antibiotic, the sharply tuned high-sensitivity portion of the tuning of auditory-nerve fibers is lost [12.51]; presumably this change reflects a similar change at the level of the basilar membrane, i. e., loss of the high-gain sharply tuned portion of the basilar-membrane response. Electrical stimulation of the MOC (Fig. 12.5), which affects only the OHC, produces similar losses in both basilar-membrane motion [12.52] and neural responses [12.53, 54]. Finally, stimulation of the MOC reduces OAE [12.55, 56]. In each case, a neural input to a cellular element of the cochlea, the OHC, affects mechanical processes in the cochlea. These data suggest that the OHCs participate in producing basilar-membrane motion. The possible mechanisms for this effect are discussed in Sect. 12.2.4.

The sound-level dependence of gain observed in Fig. 12.7b shows that the sensitivity of the cochlea is regulated across sound levels. The gain is high at low sound levels and decreases at higher sound levels; as a result, the output varies over a narrower dynamic range than the input, which is compression. A different view of compression is shown in Fig. 12.7c, which plots basilar-membrane input/output functions at various frequencies for a 10 kHz site on a chinchilla basilar membrane [12.36]. Basilar-membrane response is measured as velocity, instead of displacement as in previous figures. However, velocity and displacement are proportional for a fixed frequency, so in terms of input/output functions it does not matter which variable is plotted. Figure 12.7c has logarithmic axes, so a linear growth of response, in which the output is proportional to the input, corresponds to a line with slope 1, as for the dashed line at right. At low sound levels (< 40 dB), the response is largest at 10 kHz, as it should be for the BF. The response to 10 kHz is roughly linear at very low sound levels (< 20 dB), but has a lower slope at higher levels. Over the range of input sound levels from 20–80 dB SPL, the output velocity increases only 10-

fold or 20 dB, a compression factor of about 0.3. At lower frequencies (8 and 2 kHz), the slope is closer to 1, as expected from the constant gain at low frequencies in Fig. 12.7b. At higher frequencies (11 kHz), the growth of response is also compressive, but with a lower gain. Finally, at very high frequencies (16 kHz), the growth is again approximately linear.

The behavior shown in Figs. 12.7b,c is typical of cochleae that are judged to be in the best condition during the measurements. As the condition of the cochlea deteriorates, the input/output functions become more linear and their gain decreases [12.57], reflecting a loss of cochlear amplification. Although such data are not available for the example in Fig. 12.7c, the typical post-mortem behavior of input/output functions at BF is something like the dashed line used to illustrate linear growth. Post-mortem functions have a slope of 1 at all sound levels and typically intercept the compressive BF input/output function at levels of 70–100 dB. Assuming that the cochlear amplifier is not functioning post-mortem, the gain of the amplifier can be defined as the horizontal distance between the linear-growth portion of the BF curve in the normal ear and the post-mortem curve. With this definition of gain, the compression region of the input/output function can be understood as resulting from a gradual decrease in amplification as the sound grows louder.

The compression of basilar-membrane response shown in Fig. 12.7c has a number of perceptual correlates [12.58]. The degree of compression can be measured in human observers using a masking technique, motivated by the behavior of basilar-membrane data like Fig. 12.7 [12.59, 60]; the compression measured in these studies is comparable to that measured in basilar-membrane data. Moreover, compression can be used to explain a number of perceptual phenomena, including aspects of temporal processing and loudness growth. In hearing-impaired persons, compression is lost to varying degrees, consistent with the effects of loss of OHCs on basilar-membrane responses discussed above (i. e., the slopes of basilar-membrane input/output functions steepen). Some of the effects of hearing impairment can be explained by a change in compression ratio from 0.2–0.3 to a value near 1. An important example is loudness recruitment. If loudness is somehow proportional to the overall degree of basilar-membrane motion, then a steepening of the growth of basilar-membrane motion with sound intensity should lead to a steepening of loudness growth with intensity. This is the major effect observed on loudness growth with hearing impairment.

### Mechanisms Underlying Basilar-Membrane Tuning

The current understanding of how the properties of basilar-membrane motion arise is incomplete. Work on this subject has proceeded along two lines:

1. collection of evermore accurate data on the motion of the basilar membrane and the components of the organ of Corti; and
2. models of the observed motion of the basilar membrane based on physical principles of mechanics and fluid mechanics.

Progress in this field has been limited by the difficulty of obtaining data, however, and modelers have generally responded vigorously to each new advance in observing and measuring basilar-membrane motion. At present, the major impasse in this work seems to be the difficulty of observing the independent motion of the components of the organ of Corti. Such data are necessary to resolve questions about the mode of stimulation of hair cells by the motion of the basilar membrane and questions about the effects of OHC and stereociliary movements on the basilar membrane.

Modeling of basilar-membrane motion has been approached with a variety of methods in an attempt to account for the properties of the motion. Comprehensive reviews of this literature and its relationship to important aspects of data on basilar-membrane motion are available [12.61, 62]. The next paragraphs provide a rough summary of the current understanding of this topic.

Tuning or the separation of frequencies in basilar-membrane motion is usually attributed to the variation in the stiffness and (sometimes) the mass of the basilar membrane along its length. In most basilar-membrane models, the points on the basilar membrane are assumed to move independently; that is, the longitudinal stiffness coupling adjacent points on the membrane is assumed to be small. With this assumption, the resonant frequency of a point on the basilar membrane should vary approximately as the square root of its stiffness divided by its mass, using the usual formula for the resonant frequency of a mass–spring oscillator. In so-called long-wave models, it is this resonant frequency that determines the mapping of frequency into place in the cochlea. Experimentally, the stiffness of the basilar membrane varies from high near the base to low at the apex [12.33, 63]. Thus the stiffness gradient is qualitatively consistent with the observed place–frequency map; however, whether the stiffness gradient is sufficient

to fully account for tuning in the cochlea is not settled, because of the difficulty of making measurements.

Recent efforts in cochlear modeling have been devoted to micromechanical models, i. e., models of the detailed mechanics of the organ of Corti and the tectorial membrane [12.49, 62]. Movement of the basilar membrane is coupled to the hair cells through the organ of Corti, particularly through the relative movement of the top surface of the organ (the reticular lamina) in which the hair cells are inserted and the overlying tectorial membrane (refer to Fig. 12.4c). Mechanical feedback from the OHCs is similarly coupled into the basilar membrane through the same structures. The structure of the organ of Corti is complex and heterogeneous, with considerable variation in the stiffness of its different parts [12.64]. Thus a full account of the properties of the basilar membrane awaits an adequate micromechanical model, based on accurate data on the mechanical properties of its components.

In both models and measurements, the sound pressure difference across the basilar membrane drops rapidly to zero past the point of resonance. This behavior is illustrated by the high-frequency part of the data in Fig. 12.7b and the lack of deflection beyond the peak of the responses in Fig. 12.7a. This fact means that there is no pressure difference across the basilar membrane at the apical end of the cochlea, so the helicotrema does not affect basilar-membrane mechanics (in particular it does not *short out* the pressure difference driving the basilar membrane) except at very low frequencies, where the displacement is large near the apex. The role of the helicotrema is presumably to prevent the generation of a constant pressure difference across the basilar membrane; such a difference would interfere with the delicate transducer system in the organ of Corti.

The frequency analysis done by the basilar membrane is preserved by the arrangement of hair cells and nerve fibers in the cochlea (Fig. 12.6b). A particular hair cell senses only the local motion of the basilar membrane, so that the cochlear place map is recapitulated in the population of hair cells spread out along the basilar membrane. Moreover, each AN fiber innervates only one IHC, so the cochlear place map is again recapitulated in the AN fiber array. As a result, AN fibers that innervate, say, the 3 kHz place on the basilar membrane are maximally activated by 3 kHz energy in the sound and it is the level of activation of those fibers that provides information to the brain about the 3 kHz energy in the sound. The representation of sound in an array of neurons tuned to different frequencies is the basic or-

ganizing principle of the whole auditory system and is called *tonotopic* organization.

### 12.2.3 Representation of Sound in the Auditory Nerve

Before discussing cochlear transduction in hair cells, it is useful to introduce some properties of the responses to sound of AN fibers. Of course, the properties of AN fibers derive directly from the properties of the basilar membrane and the transduction process in IHCs. AN fibers encode sound using trains of action potentials, which are pulses fired by a fiber when stimulated by a hair-cell synapse. Information is encoded in the rate at which the fiber discharges action potentials or by the temporal pattern of action potentials. Fibers are active spontaneously at rates that vary from near 0 to over 100 spikes/s. When stimulated by an appropriate sound, the fiber's discharge rate increases and the temporal patterning of action potentials often changes as well. Figure 12.8 shows some basic features of the encoding process. Reviews of the representation of sound by auditory neurons are provided by *Sachs* [12.65], *Eggermont* [12.66] and *Moore* [12.67]. Another view is provided by recent attempts to model comprehensively the responses of AN fibers [12.68–70] or to analyze the information encoded using theoretical methods [12.71].

The tuning of the basilar membrane is reflected in the tuning of AN fibers as is shown by the tuning curves in Fig. 12.8a. This figure shows tuning curves from 11 AN fibers with different BFs. Each curve shows how intense a tone has to be (ordinate) in order to produce a criterion change in discharge rate from a fiber, as a function of sound frequency (abscissa). The tuning curves qualitatively resemble the basilar-membrane response functions shown in Fig. 12.7b for the lowest sound levels (after being turned upside down). The comparison should not be exact because the data are from different species and the tuning curves in Fig. 12.8a are constant-response contours whereas the basilar-membrane functions in Fig. 12.7b are constant-input-level response functions. However, a quantitative comparison of threshold functions for the basilar membrane and AN fibers from the same species yields a good agreement, and it is generally considered that AN tuning is accounted for by basilar-membrane tuning [12.34]. The AN consists of an array of fibers tuned across the range of frequencies that the animal can hear. The frequency content of a sound is conveyed by which fibers are activated, the tonotopic representation discussed in the previous section.

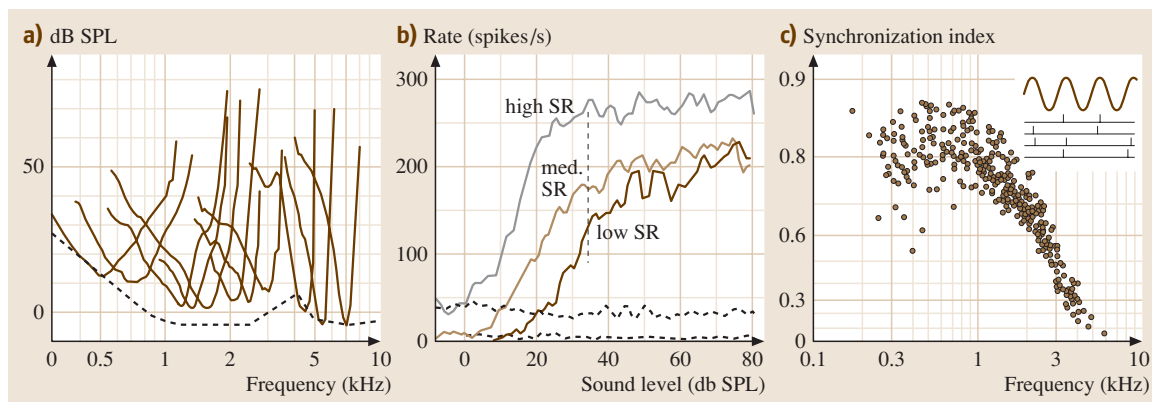


**Fig. 12.8a–c** Basic properties of responses to sound in AN fibers. **(a)** Tuning curves, showing the threshold sound level for a response plotted versus frequency. the *dashed line* shows the lowest thresholds across a population of animals. **(b)** Rate versus sound-level plots for responses to BF tones in three AN fibers. Rate in response to a 200 ms tone is shown by the *solid lines* and SR by the *dashed lines*, which actually plot the SR during the 400 ms immediately preceding each stimulus. The fibers had similar BFs (5.36, 6.18, and 5.74 kHz) but different spontaneous rates and were recorded successively in the same experimental preparation. The fluctuations in the curves derive from the randomness in the responses remaining after three-point smoothing of the curves. **(c)** Strength of phase-locking in a population of AN fibers to a BF tone plotted as a function of BF. Phase-locking is measured as the synchronization index, equal to the magnitude of the Fourier transform of the spike train at the stimulus frequency divided by the average rate. The *inset* illustrates phase-locked spike trains (Fig. 12.8a after [12.74], Fig. 12.8c after [12.75])

The perceptual sense of sound frequency, of the highness or lowness of a simple sound like a tone, is strongly correlated with stimulus frequency and, therefore, with the population of AN fibers activated by the sound. However, the pitch of a complex sound, as for musical sounds or speech, is a more complex attribute both in terms of the relationship of pitch to the physical qualities of the sound [12.72] and in terms of the representation of pitch in the AN. A discussion of this issue is provided by Cariani and Delgutte [12.73].

The intensity of a sound is conveyed by the rate at which fibers respond. AN fibers increase their discharge rates as sound intensity increases (Fig. 12.8b). In mammalian ears, fibers vary in their threshold sensitivity, where threshold means the sound level at which the rate increases from the spontaneous rate. The threshold variation is correlated with spontaneous discharge rate (SR), so that very sensitive fibers, those with the lowest thresholds, have relatively high SR and less-sensitive fibers have lower SR [12.76]. Fibers are broken into three classes, low, medium, and high, using the somewhat arbitrary criteria of 0.5–1 spikes/s to divide low from medium and 15–20 spikes/s to divide medium from high, depending on the experimenters. Figure 12.8b shows plots of discharge rate versus sound level for an example fiber in each SR group, labeled on the fig-

ure. Fibers of all SRs have similar rate-level functions; for tones, these increase monotonically with sound level (except for the effect of noisy fluctuations) from spontaneous rate to a saturation rate. In high-SR fibers, the dynamic range, the range over which sound intensity increases produce rate increases, is narrow and the saturation of discharge rate at high sound levels is clear. In low- and medium-SR fibers, the saturation is gradual (sloping) and the dynamic range is wider.

The sloping saturation in low- and medium-SR fibers is thought to reflect compression in basilar-membrane responses [12.21, 77]. High-SR fibers do not show sloping saturation because the fiber reaches its maximum discharge rate at sound levels where growth of the basilar-membrane response is linear (e.g. below 20 dB in Fig. 12.7). By contrast, the low- and medium-SR fibers sample both the linear and compressed portion of the basilar-membrane input/output function. The vertical dashed line in Fig. 12.8 shows the approximate threshold for basilar-membrane compression inferred for these fibers.

The relationship of AN responses to the perceptual sense of loudness is an apparently simple problem that has not been fully solved. While it is generally assumed that loudness is proportional to the overall increase in discharge rate across all BFs [12.78], this

calculation does not predict important details of loudness growth [12.79–81], especially in ears with damage to the hair cells. Presumably there are additional transformations in the central auditory system that determine the final properties of loudness growth.

A property of AN discharge that is important for many sounds is the ability to represent the temporal waveform. Sounds such as speech have information encoded at multiple levels of temporal precision [12.82]; these include

1. syllables and other aspects of the envelope at frequencies below 50 Hz;
2. periodicity (pitch) in sounds such as vowels at frequencies from 50–500 Hz; and
3. the fine structure of the actual oscillations in the acoustic waveform at frequencies above 500 Hz.

AN fibers represent the waveform of sounds (the fine structure) by phase-locking to the stimulus. A schematic example is shown in the inset of Fig. 12.8c, which shows a sinusoidal acoustic waveform (a tone) and four examples of AN spike trains in response to the stimulus. The important point is that the spikes in the responses do not occur at random, but rather at a particular stimulus phase, near the positive peak of the stimulus waveform in this example. The phase-locking is not perfect, in that a spike does not occur on every cycle of the stimulus, and the alignment of spikes and the waveform varies somewhat. However, a histogram of spike-occurrence times shows a strong locking to the stimulus waveform and the Fourier transform of the spike train generally has its largest component at the frequency of the stimulus.

Phase-locking occurs at stimulus frequencies up to a few kHz, depending on the animal. The main part of Fig. 12.8c shows the strength of phase-locking in terms of the synchronization index (defined in the caption) plotted against the frequency of the tone. These data are from the cat ear [12.75] where phase-locking is strongest below 1 kHz and disappears by about 6 kHz. Phase-locking always shows this low-pass property of being strong at low frequencies and nonexistent at high frequencies. The highest frequency at which phase-locking is seen varies in different species, being lower in rodents than in cats [12.83].

AN phase-locking is essential for the perception of sound localization. The relative time of occurrence of spikes from the two ears is used to compute the delays in the stimulus waveform across the head that provide information about the azimuth of a sound source [12.84]. Phase-locking has also been suggested as a basis for processing of speech and other complex

stimuli [12.71,85]. Examples of the usefulness of phase-locking in analyzing responses to complex stimuli are given in Sect. 12.3.1.

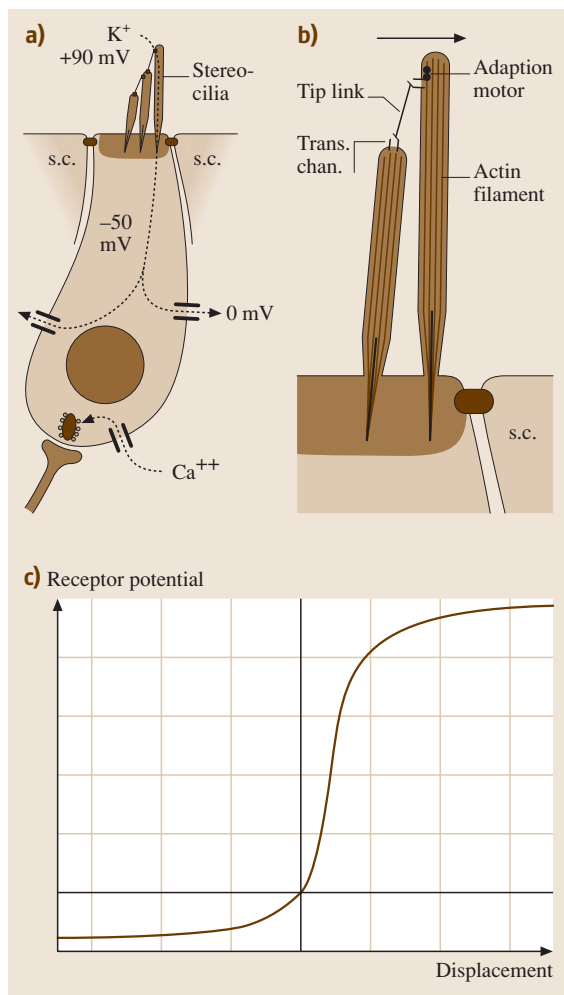
## 12.2.4 Hair Cells

The transduction of basilar-membrane motion into electrical signals occurs in the IHCs. The OHCs participate in the generation of sensitive and sharply tuned basilar-membrane motion. In this section, the physiology of IHCs and OHCs are described with reference to these tasks. At the time of this writing, hair-cell research is one of the most active areas in auditory neuroscience and many of the details of hair-cell function are just being worked out. Useful recent reviews of the literature are available [12.86–89].

### IHCs and Transduction

Both IHCs and OHCs transduce the motion of the basilar membrane. This section describes transduction with reference to the IHCs, but transduction works in essentially the same fashion in OHCs. The transduction apparatus depends on the arrangement of stereocilia on the apical surface of hair cells. Stereocilia are structures that protrude from the hair cells into the endolymphatic space of the SM (Fig. 12.9a). They consist of bundles of actin filaments anchored in an actin/myosin matrix just under the apical surface of the cell. The membrane of the cell wraps the actin rods so that they are intracellular and the membrane potential of the cell appears across the membranes of the stereocilia. The structure of stereocilia is intricate and involves a number of structural proteins that are important for organizing the development of the cilia and for maintaining them in proper position on the cell [12.90]. The stereocilia form a precisely organized bundle; in the cochlea, the bundle consists of several roughly V- (IHCs) or W-shaped (OHCs) rows of cilia (typically three, as in Fig. 12.9) of graded length, so that the cilia in the row nearest the lateral edge of the hair cell are the longest and those in the adjacent rows are successively shorter. Each row consists of 20–30 cilia precisely aligned with the cilia in adjacent rows. The tips of the cilia are connected by tip links [12.91], a string-like bundle of protein that connects the tip of a shorter cilium to the side of the taller adjacent cilium (Fig. 12.9b).

Transduction occurs when vertical motion of the basilar membrane is converted into a shearing motion of the stereocilia (the arrow in Fig. 12.9b). It has long been known that hair cells are functionally polarized, in the sense that they respond most strongly to displacement of the cilia in the direction of the arrow, are



inhibited by displacement in the opposite direction, and respond weakly to displacement of the cilia in lateral directions [12.92, 93]. In fact, hair cells are depolarized when the stereocilia are displaced in the direction that stretches the tip links. Further evidence to associate the tip links to the transduction process is that when the tip links are destroyed by lowering the extracellular calcium concentration, transduction disappears and reappears as the tip links are regenerated [12.94].

The mechanical connection between basilar-membrane motion and cilia motion is not fully understood. As shown in Fig. 12.4c, the stereocilia bundles are oriented so that lateral displacement of the cilia (i. e., displacement away from the central axis of the cochlea) should be excitatory. Furthermore the tips of the OHC cilia are embedded in the tectorial membrane, whereas those of

**Fig. 12.9a–c** Transduction in IHCs. **(a)** Schematic of an IHC showing the components important for transduction. The stereocilia protrude into the endolymphatic space (*top*), containing mainly  $K^+$ ; the extracellular potential here is about +90 mV (the endolymphatic potential). The transduction apparatus consists of tip links and channels near the tips of the cilia. The *dashed lines* show the transduction current. It enters the cell through the transduction channel and exits through  $K^+$  channels in the basolateral membrane of the cell into the perilymphatic space. The intracellular and extracellular potentials of the cell and the perilymphatic space are given. There is a mechanically stiff and electrically insulating boundary between the endolymphatic and perilymphatic spaces, formed by tight junctions between the apical surfaces of hair cells and supporting cells (*s.c.*), indicated by the *small black ovals*. The synapse, at the base of the cell, is a standard chemical synapse, in which voltage-gated  $Ca^{2+}$  channels open in response to the depolarization caused by the transduction current and admit  $Ca^{2+}$  to activate neurotransmitter release. **(b)** Detailed view of two stereocilia with a tip link connecting ion channels in the membrane of each. The upper ion channel is connected to an adaptation motor that moves up and down along the actin filaments to tension the tip link. **(c)** Transduction function showing the receptor potential (the depolarization or hyperpolarization) of a hair cell versus the displacement of the stereocilia tips. Typical axis scales would be 0.01–1  $\mu\text{m}$  per tick on the abscissa and  $\approx 2$  mV per tick on the ordinate

the IHC are not. Based on the geometry of the organ, upward motion of the basilar membrane (i. e., away from the ST and toward the SM and SV) results in lateral displacement of the cilia through the relative motions of the organ of Corti and the tectorial membrane. Presumably the coupling to the OHC is a direct mechanical one, whereas the coupling to the IHC is via fluid movements, so the IHC stereocilia are bent through viscous drag of the endolymph in the space between the organ of Corti and the tectorial membrane. While this model is commonly offered and is probably basically correct, it is not consistent in detail with the phase relations between the stimulus (or basilar-membrane motion) and action potential phase locking in AN fibers [12.95]. Presumably the inconsistencies reflect complexities in the motions of the organ of Corti that connect basilar-membrane displacement to stereociliary displacement.

The current model for the tip link and transduction channel is shown in Fig. 12.9b. The tip link connects (probably) two transduction channels, one in each cilium. When the bundle moves in the excitatory direction (the direction of the arrow), the tension in the tip link



increases, which opens the transduction channels and allows current flow into the cell. Movement in the opposite direction relaxes the tension in the tip link and allows the channels to close. The current through the transduction channels is shown by the dashed line in Fig. 12.9a. Outside of the stereociliary membrane is the endolymph of the SM. The transduction channels are nonspecific channels which allow small cations to pass; in the cochlea, these are mainly  $\text{Na}^+$ ,  $\text{K}^+$ , and  $\text{Ca}^{2+}$ . However, the predominant ion in both the extracellular (endolymph) and intracellular spaces is  $\text{K}^+$ , so the transduction current is mostly  $\text{K}^+$ . The energy source producing the current is the potential difference between the SM (the endolymphatic potential, approximately +90 mV) and the intracellular space in the hair cell (approximately -50 mV). The endolymphatic potential is produced by the active transport of  $\text{K}^+$  into the endolymph and  $\text{Na}^+$  out of the endolymph in the stria vascularis (Fig. 12.4b). This transport process also produces the endolymphatic potential [12.22]. The negative potential inside the hair cell is produced by the usual mechanisms in which active transport of  $\text{K}^+$  into the cell and  $\text{Na}^+$  out of the cell produces a negative diffusion potential through the primarily  $\text{K}^+$  conductances of the hair cell membrane. Because the transduction current is primarily  $\text{K}^+$ , it does not burden the hair cell with the necessity for additional active transport of ions brought into the hair cell by transduction.

When the transduction channels open, the hair cell is depolarized by the entry of positive charge into the cell. The transduction current flows out of the cell through the potassium channels in its membrane. Figure 12.9c shows the typical transduction curve for a cochlear hair cell, as the depolarization of the membrane (ordinate) produced by a certain displacement of the stereociliary bundle (abscissa). At rest (zero displacement), some transduction channels are open, so that both positive and negative displacements of the bundle can be signaled. However, hair cells generally have only a fraction of channels open at rest so that a much larger depolarization is possible than hyperpolarization, i. e., more channels are available for opening than for closing. The transduction curve saturates when all channels are closed or all channels are open.

The transduction process is completed by the opening of voltage-gated  $\text{Ca}^{2+}$  channels in the hair cell membrane, which allows  $\text{Ca}^{2+}$  ions to enter the cytoplasm (dotted line at the bottom of Fig. 12.9a) and activate the synapse. The hair-cell synapse has an unusual morphology, containing a synaptic ribbon surrounded by vesicles [12.96,97]. This ribbon presumably

reflects molecular specializations that allow the synapse to be activated steadily over a long period of time without losing its effectiveness and also to produce an action potential in the postsynaptic fiber on each release event, so that summation of postsynaptic events is not necessary, as is required for phase-locking at kilohertz frequencies. The synapse appears to be glutamatergic [12.98] with specializations for fast recovery from one synaptic release, also necessary for high-frequency phase-locking.

The final component of the transduction apparatus is the adaptation motor, shown as two black circles in Fig. 12.9b [12.99]. Presumably the transduction channel and the adaptation motor are mechanically linked together so that when the motor moves, the channel moves also. The sensitivity of the transduction process depends on having an appropriate tension in the tip link. If the tension is too high, the channels are always open; if the tip link is slack, then the threshold for transduction will be elevated because larger motions of the cilia will be required to open a transduction channel. The tip-link tension is adjusted by a myosin motor that moves upward along the actin filaments when the transduction channel is closed. When the channel opens,  $\text{Ca}^{2+}$  flows into the stereocilium through the transduction channel and causes the motor to slip downward. Thus the adaptation motor serves as a negative feedback system to set the resting tension in the tip link. The zero-displacement point on the transduction curve in Fig. 12.9c is set by an equilibrium between the motor's tendency to climb upward and the tension in the tip link, which causes the channel to open and admit  $\text{Ca}^{2+}$ , pulling it downward. Adaptation also regulates the sensitivity of the transduction process in the presence of a steady stimulus.

There is a second, fast, mechanism for adaptation in which  $\text{Ca}^{2+}$  entering through an open transduction channel acts directly on the channel to close it, thus moving the transduction curve in the direction of the applied stimulus [12.88]. This mechanism is discussed again in a later section, because it also can serve as a kind of cochlear amplifier.

### IHC Transduction and the Properties of AN Fibers

The description of transduction in the previous section suggests that the stimulus to an AN fiber should be approximately the basilar-membrane motion at the point in the cochlea where the IHC innervated by the fiber is located. It follows that the tuning and rate responses of the fiber should be similar to the tuning and response amplitude of the basilar membrane, discussed in connection with Fig. 12.7.

The receptor potentials in an **IHC** responding to tones are shown in Fig. 12.10 [12.83]. The traces are the membrane potentials recorded in an **IHC**, each trace at a different stimulus frequency. These potentials are the driving force for the  $\text{Ca}^{2+}$  signal to the synapse, and thus indirectly for the **AN** fibers connected to the cell. The properties of these potentials can be predicted from Fig. 12.9c by the thought experiment of moving a stimulus sinusoidally back and forth on the abscissa and following the potential traced out on the ordinate. The potential should be a distorted sinusoid, because

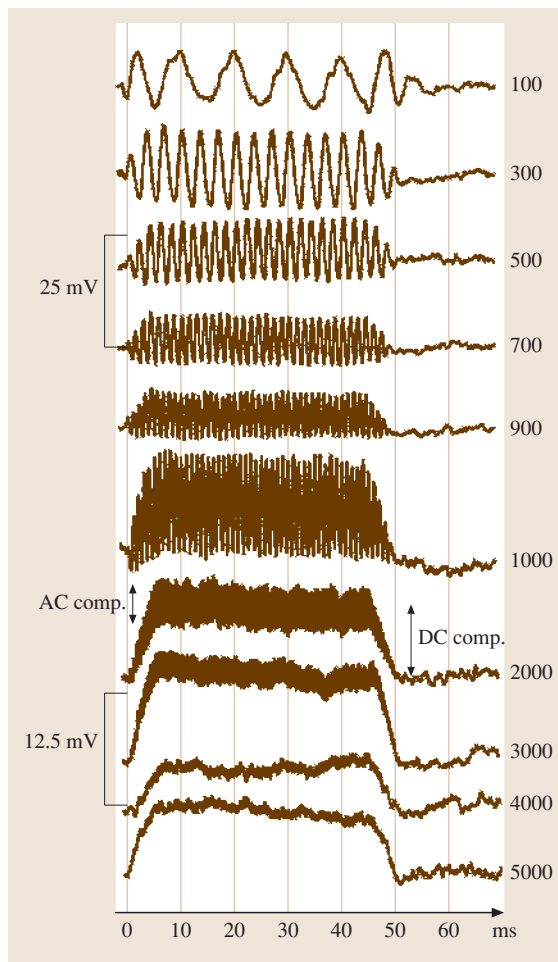


**Fig. 12.10** Receptor potentials in an **IHC** in the basal turn of a guinea-pig cochlea. The stimulus level was set at 80 dB SPL so that the cell would respond across a wide range of frequencies. Stimulus frequency is given at right. Notice the change in ordinate scale between the 900 Hz and 1000 Hz traces. (After [12.83], with permission)

depolarizing responses are larger than hyperpolarizing ones, and it should have a steady (DC) offset, also because of the asymmetry favoring depolarization. At low frequencies, both components can be seen in Fig. 12.10; the response is a distorted sinusoid riding on a steady depolarization. At high frequencies ( $>1000$  Hz), the sinusoidal component is reduced by low-pass filtering by the cell's membrane capacitance and only the steady component is seen. The transition from sinusoidal receptor potentials at low frequencies to rectified DC potentials at high frequencies corresponds to the loss of phase-locking at higher frequencies in **AN** fibers (Fig. 12.8c). At low frequencies, the **IHC/AN** synapse releases transmitter on the positive half cycles of the receptor potential and the **AN** fiber is phase-locked; at high frequencies, there is a steady release of neurotransmitter and the **AN** fiber responds with a rate increase but without phase-locking.

#### OHCs and the Cochlear Amplifier

In the discussion of the basilar membrane, the need for a source of energy in the cochlea, a cochlear amplifier, was discussed. At present, two possible sources of the amplification have been suggested. The first is **OHC** motility [12.86, 100] and the second is hair bundle motility [12.101]. Although hair bundle motility could function in both **IHCs** and **OHCs**, it seems likely that

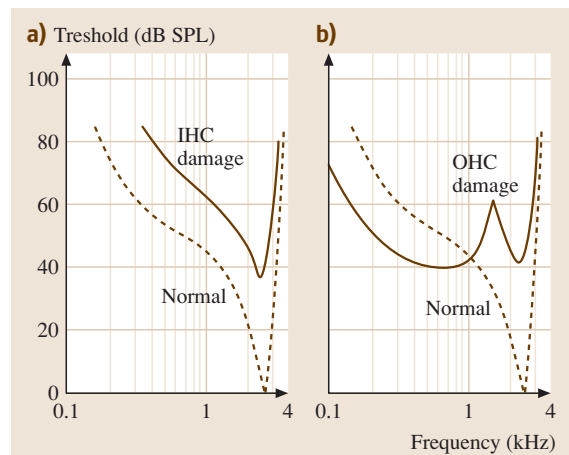


**Fig. 12.11a,b** Schematic summary of **AN** tuning curves in normal ears and in ears with damaged cochleae. **(a)** In regions of the cochlea with remaining **OHCs** but damaged **IHCs** tuning curves mainly show a threshold elevation. **(b)** In regions with missing **OHCs** but intact **IHCs** there is an elevation of threshold at frequencies near **BF** and a substantial broadening of tuning. (After [12.51])

the **OHC** is the principal element of the cochlear amplifier. The evidence for this is that the properties of the cochlea change in a way consistent with modification of cochlear mechanics when the **OHC** are damaged or otherwise manipulated, but not the **IHC**. For example, electrical stimulation of the **MOC**, which projects only to the **OHCs** (Fig. 12.5), modifies otoacoustic emissions [12.31] and reduces the amplitude of motion of the basilar membrane [12.102, 103].

Figure 12.11 shows tuning curves in **AN** fibers for intact ears (“normal”) and for ears with **IHC** or **OHC**

damage [12.51, 105]. These tuning curves are schematics that summarize the results of studies in ears with damage due to acoustic trauma or ototoxic antibiotics. Complete destruction of **IHCs**, of course, eliminates **AN** activity entirely. However, it is possible to find regions of the cochlea with surviving **IHCs** that have damaged stereocilia and **OHCs** that appear intact. The sensitivity of **AN** fibers in such regions is reduced, reflected in the elevated threshold in Fig. 12.11a, but the tuning is still sharp and appears to be minimally altered. By contrast, in regions with intact **IHCs** and **OHCs** that are damaged or missing, the tuning curves are dramatically altered, as in Fig. 12.11b. There is a threshold shift reflecting a loss of sensitivity but also a substantial broadening of tuning. These are the effects that are expected from the loss of the cochlear amplifier. Note that the thresholds well below **BF** (<1 kHz in Fig. 12.11b) can actually be lower than normal with **OHC** damage. This phenomenon is not fully understood and seems to reflect the existence of two modes of stimulation of **IHCs** [12.106].

Some properties of **OHCs** are shown in Fig. 12.12. These cells have a transduction apparatus similar to that in **IHCs**, but Fig. 12.12 focuses on unique aspects of **OHC** anatomy and physiology. The **OHCs** are located in an unusual system of structural or supporting cells. Unlike virtually all tissues, the **OHC** are surrounded by a fluid space containing perilymph for distances comparable to the cells’ widths (asterisks in Fig. 12.4c). The **OHC** are held by supporting cells called Deiter’s cells

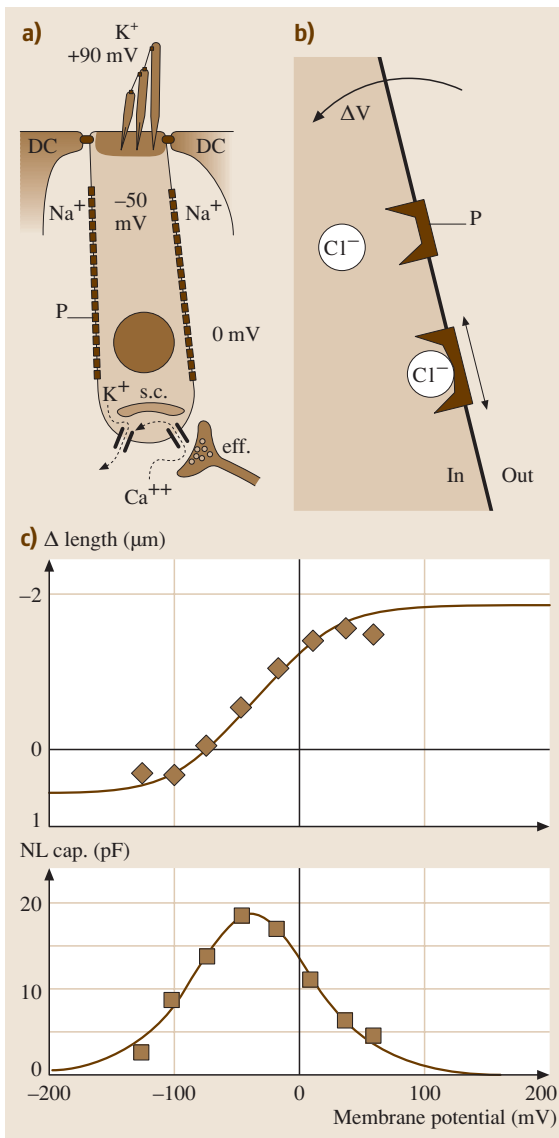


**Fig. 12.12** (a) Schematic picture of an **OHC** showing elements important for **OHC** function. The diagram is labeled as for Fig. 12.9a except for the following: DC – Deiter’s cell extensions that are linked to **OHCs** by tight junctions to form the top surface of the organ of Corti;  $\text{Na}^+$  – the extracellular spaces around the lateral membranes of the **OHCs** are filled with perilymph, a high- $\text{Na}^+$ , low- $\text{K}^+$  fluid; P – prestin molecules in the lateral membrane; eff. – efferent terminal of a **MOC** neuron on the **OHC**; s.c. subsynaptic cistern associated with the efferent synapse.  $\text{K}^+$  and  $\text{Ca}^{2+}$  currents activated by the synapse are shown by dashed and dotted lines, respectively. (b) Schematic of prestin molecules in the lateral membrane of the cell. When the membrane potential  $\Delta V$  is negative,  $\text{Cl}^-$  ions are driven into the prestin molecule, increasing its membrane area (as indicated by the double-headed arrow). (c) The top plot shows the length of an isolated **OHC** as a function of membrane potential showing the amplitude of the electromotility. The bottom plot shows the nonlinear capacitance of the same cell. (Fig. 12.12c after [12.104] with permission)

that form a cup around the base of the cell and have a stiff extension up to the top surface of the organ of Corti. The extension terminates next to the apical surface of the **OHC**, where a system of tight junctions similar to that in the **IHC** region holds the **OHCs** and Deiter's cells to form a mechanically stiff and electrically insulating barrier between the endolymph and perilymph.

In response to depolarization of their membranes, say in response to a transduction current, **OHCs** shorten, a process called electromotility [12.107, 108]. Electromotility does not use a direct chemical energy source [such as adenosine triphosphate (ATP)] as do other cellular motility processes. It is also very fast, responding to frequencies of 10 kHz or above, limited mainly by the limits of the experimental observations. This unusual motile process is produced by a molecule called prestin ("P" in Fig. 12.12a) found in a dense array in the lateral wall of the **OHCs** [12.109–111], where it is associated with a complex mechanical matrix that forms the cell's skeleton [12.112]. Prestin causes the cell to shorten in response to electrical depolarization of its membrane, so the energy source for electromotility is the electrical membrane potential. The mechanism of electromotility is shown schematically in Fig. 12.12b. The prestin molecule is similar to anion transporters, molecules that normally move anions through the cell membrane. It is thought that prestin is a modified transporter that can bind an anion, but the ion moves only part of the way through the membrane. In **OHCs**, the relevant anion is  $\text{Cl}^-$  because electromotility is blocked by removing  $\text{Cl}^-$  from the cytoplasm [12.113]. When a  $\text{Cl}^-$  ion binds to a prestin molecule, the cross-sectional area of the molecule increases, thus increasing the membrane area and lengthening the cell (indicated by the double-headed arrow).  $\text{Cl}^-$  ions are driven into the membrane by negative membrane potentials, so depolarization pulls them out and decreases the membrane area, shortening the cell.

When a  $\text{Cl}^-$  ion binds to a prestin molecule, it moves part way through the cell's electrical membrane potential ( $\Delta V$  in Fig. 12.12b). This movement behaves like charging a capacitance in the cell's membrane and appears in electrical recordings as an additional membrane capacitance. However the extent of charge movement depends on the membrane potential, making the capacitance nonlinear. At very negative membrane potentials, all the prestin molecules have a bound  $\text{Cl}^-$  and no charge movement can occur; similarly, at positive potentials, the  $\text{Cl}^-$  is unlikely to bind to prestin and again no charge movement can occur. Thus the nonlinear capacitance is significant only over the range of membrane potentials where the prestin molecules are partially bound to

$\text{Cl}^-$ . The bottom part of Fig. 12.12c shows the nonlinear capacitance as a function of membrane potential, showing the predicted behavior [12.104]. The top part of Fig. 12.12c shows the electrically produced change in cell length; as expected, changes in cell length are observed only over the range of membrane potentials where the nonlinear membrane capacitance is observed.

Prestin is found essentially only in **OHCs** and, in particular, is not seen in **IHCs** [12.111]. When expressed by genetic methods in cells that normally do not contain it, prestin confers electromotility on those cells. In addition, when the prestin gene was knocked out, the morphology of the cochlea and the hair cells was not affected (except that the **OHCs** were shorter), but electromotility was not observed and the sensitivity of auditory neurons was decreased; otoacoustic emissions were also decreased [12.114]. These are the effects expected if prestin is the energy source for the cochlear amplifier.

The means by which **OHC** motility amplifies basilar-membrane motion is somewhat uncertain. Models that use physiologically accurate **OHC** motility to produce cochlear amplification have been suggested and analyzed, e.g., [12.115]. However, such models require assumptions about the details of the mechanical interactions within the organ of Corti, assumptions that have not been tested experimentally. For example, the **OHCs** lie at an angle to the vertical extensions of the Deiter's cells, so that successive locations along the basilar membrane are coupled to one another [12.108]. The mechanical effects of structures like this are quite important in models of basilar-membrane movement that incorporate **OHC** electromotility [12.62]. An additional major uncertainty at present about a prestin-derived cochlear amplifier is the fact that prestin depends on the membrane potential as its driving signal [12.88]. Because the membrane potential is low-pass filtered by the cell's membrane capacitance, in the fashion seen in Fig. 12.10, it is not clear that a prestin-based mechanism can generate sufficient force at high frequencies.

The second possible mechanism for the cochlear amplifier is by stereocilia bundle movements that can amplify hair-cell stimulation either through nonlinearities in the compliance of the bundle or through active hair-bundle movements [12.89, 101]. Essentially these mechanisms work by moving the bundle further in the direction of its displacement, which would amplify the stimulation of the hair cell. Calculations suggest that the speed of bundle movement is sufficient and that the stiffness of the bundles is a significant fraction of the basilar-membrane stiffness, both necessary conditions for a stereociliary-bundle motor to be the cochlear ampli-

fier. Of course both the prestin and stereociliary-bundle mechanisms may operate.

The final aspect of OHC physiology shown in Fig. 12.12a is the efferent synapse made by the MOC neuron on the OHC. This synapse activates an unusual cholinergic postsynaptic receptor which admits a significant  $\text{Ca}^{2+}$  current (dotted line), along with other cations, to the cytoplasm. The  $\text{Ca}^{2+}$  current activates a calcium-dependent potassium channel producing

a larger potassium current (dashed line) [12.116]. The efferent synapse inhibits OHC function, decreasing the sensitivity of AN fibers and broadening their tuning, effects consistent with a decrease in cochlear amplification [12.31]. The mechanism is thought to be an increase in the membrane conductance of the OHC, from opening the calcium-dependent  $\text{K}^+$  channel, which hyperpolarizes the cell and shorts the transducer current, producing a smaller receptor potential.

## 12.3 Auditory Nerve and Central Nervous System

In a previous section, the basic properties of AN fiber responses to acoustic stimuli were described. These properties can be related directly to the properties of the basilar membrane and hair cells. The auditory system does not usually deal with the kinds of simple stimuli that have been considered so far, i. e., tones of a fixed frequency. When multiple-tone complexes or other stimuli with multiple frequency components are presented to the ear, there are interactions among the frequency components that are important in shaping the responses. This section describes two such interactions and then provides an overview of the tasks performed by the remainder of the auditory system.

### 12.3.1 AN Responses to Complex Stimuli

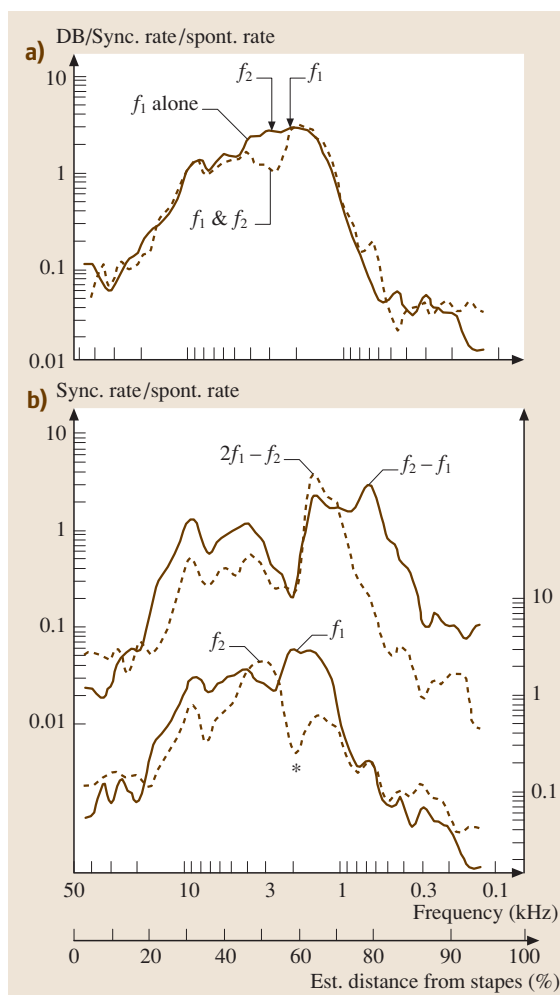
Many of the features of responses of AN fibers to complex stimuli can be seen from the responses to a two-tone complex. An example is shown in Fig. 12.13 which shows responses of AN fibers to 2.17 and 2.79 kHz tones (called  $f_1$  and  $f_2$ , respectively) presented simultaneously and separately [12.117]. In this experiment a large population of AN fibers were recorded in one animal and the same set of stimuli were presented to each fiber. Because fibers were recorded across a wide range of BFs, this approach allows the construction of an estimate of the response of the whole AN population. Responses are plotted in Fig. 12.13 as the strength of phase-locking to various frequency components of the stimulus. Phase-locking is used here to allow the complex responses of the fibers to be separated into responses to the various individual frequency components. The abscissa is plotted as BF, on a reversed frequency scale, and also in terms of the distance of the fibers' points of innervation from the stapes.

The distribution of responses to the  $f_1$  frequency component (2.17 kHz) presented alone is shown in

Fig. 12.13a by the solid line. The response peaks near the point of maximum response to  $f_1$ , indicated by the arrow labeled  $f_1$  at the top of the plot. The dotted line shows the phase-locking to  $f_1$  when the stimulus is a simultaneous presentation of  $f_1$  and  $f_2$ . The response to  $f_1$  is similar in both cases, except near the point of maximum response to  $f_2$  (at the arrow marked  $f_2$ ) where the response to  $f_1$  is reduced by the addition of  $f_2$  to the stimulus. This phenomenon is called two-tone suppression [12.118, 119]; it can be suppression of phase-locking as in this case or it can be a decrease of the discharge rate in response to an excitator tone when a suppressor tone is added. Suppression can be seen on the basilar membrane as a reduction in the membrane motion at one frequency caused by the addition of a second frequency [12.34], and is usually explained as resulting from compression in the basilar-membrane input/output relationship.

The importance of suppression for responses to complex stimuli is that it improves the tonotopic separation of the components of the stimulus. In Fig. 12.13a, for example,  $f_1$  presented by itself (solid line) gives a broad response that spreads away from the  $f_1$  place and encompasses the  $f_2$  place. In the presence of  $f_2$ , the  $f_1$  response is confined to points near the  $f_1$  place, thus improving the effective tuning of the fibers for  $f_1$ . The bottom part of Fig. 12.13b shows that the responses at the  $f_2$  place are dominated by phase-locking to  $f_2$  when  $f_1$  and  $f_2$  are presented simultaneously (dashed curve). The suppression effect is symmetric and a dip in the response to  $f_2$  is observed at the  $f_1$  place (at the asterisk in the bottom plot of Fig. 12.13b) which represents suppression of  $f_2$  by  $f_1$ .

The top part of Fig. 12.13b shows responses to combination tones, another phenomenon that can be important in responses to complex stimuli. When two tones are presented simultaneously, observers can hear



distortion tones, most strongly at the cubic distortion frequency  $2f_1 - f_2$  (1.55 kHz here). This distortion component is produced in the cochlea and is a prominent part of otoacoustic emissions for two-tone stimuli. It is used for both diagnostic and research purposes as a measure of OHC function [12.46]. In the cochlea, phase-locking at the frequency  $2f_1 - f_2$  is seen, as shown by the dotted curve in the top part of Fig. 12.13b. It is important that the response to  $2f_1 - f_2$  peaks at the place appropriate to the frequency  $2f_1 - f_2$  (indicated by the arrow). The distribution of phase-locking to  $2f_1 - f_2$  is similar to the distribution of phase-locking to a single tone at the frequency  $2f_1 - f_2$ , when account is taken of suppression effects and of sources of distortion in the region near the  $f_1$  and  $f_2$  places [12.117]. This behavior has been interpreted as showing that cochlear nonlin-

**Fig. 12.13a,b** Responses of a population of AN fibers to a two-tone complex consisting of  $f_1=2.17$  kHz and  $f_2=2.79$  kHz at 65 dB SPL. The ordinates show the strength of the phase-locked response as the synchronized rate divided by the spontaneous rate. Synchronized rate is the Fourier transform of the spike train at the appropriate frequency normalized to have units of spikes/s. Responses of a representative sample of fibers of different BFs were recorded. The lines are smoothed versions of the data computed as a moving-window average of the responses of individual fibers, for fibers with  $SR > 15$  /s. (a) Phase-locking to  $f_1$  for responses to the  $f_1$  stimulus tone alone (solid line) and to both  $f_1$  and  $f_2$  (dashed line). The arrows at top show the BF places for the two frequencies. (b) The top plots and left ordinate show phase-locking to the combination frequencies  $2f_1 - f_2$  (dashed) and  $f_2 - f_1$  (solid) when the stimulus was  $f_1$  and  $f_2$ . The bottom plots and the right ordinate show phase-locking to  $f_1$  (solid) and  $f_2$  (dashed). For both plots, data were taken only from fibers to which all the stimuli shown were presented. Thus the  $f_1$  phase-locking in (a) (dashed line) and in the bottom part of (b) (solid line) differ slightly, even though they estimate the same response to the same stimulus, because they were computed from somewhat different populations of fibers. (After [12.117] with permission)

earities in the region of the primary tones ( $f_1$  and  $f_2$ ) lead to the creation of energy at the frequency  $2f_1 - f_2$ , which propagates on the basilar membrane in a fashion similar to an acoustic tone of that frequency presented at the ear. The phase of the responses (not shown) is consistent with this conclusion.

There is also a distortion tone at the frequency  $f_2 - f_1$  (solid line in the top part of Fig. 12.13b), which appears to propagate on the basilar membrane and shows a peak of phase-locking at the appropriate place. This difference tone can also be heard by observers; however, there are differences in the rate of growth of the percept of  $f_2 - f_1$  versus  $2f_1 - f_2$ , such that the former grows nonlinearly and the latter linearly as the level of  $f_1$  and  $f_2$  are increased. As a result,  $f_2 - f_1$  is audible at high sound levels only.

Responses to a somewhat more complex stimulus are shown in Fig. 12.14, in this case an approximation to the vowel /eh/, as in “met” [12.65]. The magnitude spectrum of the stimulus is shown in Fig. 12.14a. It consists of the harmonics of a 125 Hz fundamental with their amplitudes adjusted to approximate the spectrum of /eh/. The actual vowel has peaks of energy at the resonant frequencies of the vocal tract, called formants; these are indicated by F1, F2, and F3 in Fig. 12.14a. Again the ex-

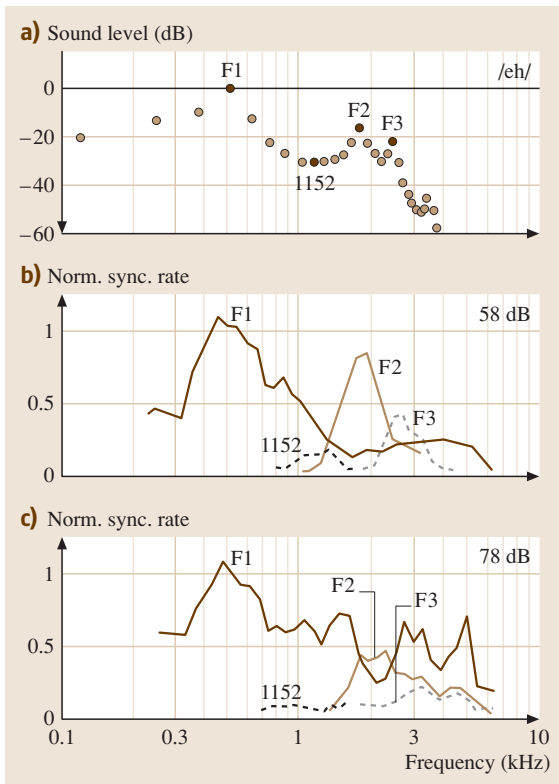


**Fig. 12.14a–c** Responses to a stimulus similar to the vowel /eh/ presented at two sound levels in a population of AN fibers. **(a)** The magnitude spectrum of the stimulus. It is periodic and consists of harmonics of a 125 Hz fundamental. There are peaks of energy at the formant frequencies of a typical /eh/, near 0.5 (F1), 1.75 (F2), and 2.275 kHz (F3). The 1.152 kHz component in the trough between F1 and F2 is used for comparison in parts **(b)** and **(c)**. **(b)** Distribution of phase-locking to four frequency components of the vowel when presented at 58 dB SPL, as labeled. These are moving-window averages of the phase-locking of individual fibers. Phase-locking here is the magnitude of the Fourier transform of the spike train at the frequency of interest normalized by the maximum discharge rate of the fiber. Maximum rate is the rate in response to a BF tone 50 dB above threshold. **(c)** Same for responses to the vowel at a sound level of 78 dB SPL. (After [12.120, 121])

perimental approach is to record from a large population of AN fibers in one animal and present the same stimulus to each fiber. The response of the whole population is estimated by a moving average of the data points for individual fibers. This stimulus contains many frequency components, so the responses are quite complex. How-

ever, the data show that formant frequencies dominate the responses. Note that combination tones always occur at the frequency of a real acoustic stimulus tone for a harmonic series like this, so it is not possible to analyze combination tones without making assumptions that allow the responses to combination and real tones to be separated [12.120].

The distribution of phase-locking in response to the formants and to one non-formant frequency are shown in Figs. 12.14b and 12.14c; these show responses at two sound levels. At 58 dB (Fig. 12.14b), the formant responses are clearly separated into different populations of fibers, so that the response to a formant is largest among fibers with BFs near the formant frequency. There are significant responses to all three formants, but there is little response to frequency components between the formants, such as the response to 1.152 kHz (dotted line). These results demonstrate a clear tonotopic representation of the vowel.

At 78 dB (Fig. 12.14c), the responses to F2 and F3 decrease in amplitude and the response to F1 spreads to occupy almost the entire population. This behavior is typically observed at high sound levels, where the phase-locking to a large low-frequency component of the stimulus spreads to higher BFs in the population [12.122]. Suppression plays two roles in this process. First, the spread of F1 and the decrease in response to F2 and F3 behave quantitatively like suppression of a tone at F2 or F3 by a tone at F1 and therefore seem to represent suppression of F2 and F3 by F1 [12.121]. Second, the response to F1 is suppressed among fibers with BFs near F2, as shown by dips in the phase-locking to F1 near the F2 place. Suppression acts to improve the representation in the latter case, but has the opposite effect in the former case.

### 12.3.2 Tasks of the Central Auditory System

The discussion so far concerns only the most basic aspects of physiological acoustics. The representation of sound in the AN is the input to a complex of neural pathways in the central auditory system. Discussion of specifics of the central processing of auditory stimuli is beyond the scope of this chapter. However, several recent books provide comprehensive coverage of the anatomy and physiology of this system, e.g., [12.123–126].

The representation of the auditory stimulus provided to the brain by the AN is a spectrotemporal one. That is, the responses of AN fibers provide an accurate representation of the moment-by-moment distribution of energy across frequency for the sound entering the ear.

In terms of processing sound, the major steps taken in the cochlea are frequency analysis, compression, and suppression. Frequency analysis is essential to all of the processing that follows in the brain. Indeed central auditory centers are all organized by frequency and most properties of the perception of sound appear to include frequency analysis as a fundamental component. Compression is important for extending the dynamic range of hearing. Its importance is illustrated by the problems of loudness abnormality and oversensitivity to loud sounds in persons with damaged cochleae that are missing compression [12.127]. Suppression is important for maintaining the quality of the spectrotemporal representation, at least at moderate sound levels, and is the first example of interaction across frequencies in the auditory system. In the following paragraphs, some of the central nervous system's secondary analyses on the cochlear spectrotemporal representation are described.

The first function of the central auditory system is to stabilize the spectrotemporal representation provided in the AN. As shown in Fig. 12.14, the representation changes across sound level and the quality of the representation is generally lower at high sound levels and at low sound levels. In the cochlear nucleus the representation is more stable as sound level changes, e.g., for speech [12.128]. Presumably the stabilization occurs through optimal combination of information across SR groups in the AN and perhaps also through inhibitory interactions.

A second function of the lower central auditory system is binaural interaction. The location of sound sources is computed by the auditory system from small

differences in the sounds at the two ears [12.84, 129]. Essentially, a sound is delayed in reaching the ear on the side of the head away from the source and is less intense there. Differences in interaural stimulus timing are small and require a specialized system of neurons in the first and second stages of the central auditory system to allow accurate representation of the interaural timing cues. A similar system is present for interaural differences in sound level. The representation of these cues is elaborated in higher levels, where neurons show response characteristics that might explain perceptual phenomena like binaural masking level differences [12.130] and the precedence effect [12.131].

A third aspect of central processing is that the representation of sound switches away from a spectrotemporal description of the stimulus, as in the AN, and moves to derived representations, such as one that represents auditory objects [12.132]. For example, the representation of speech in the auditory cortex does not take a recognizable tonotopic form, in that peaks of activity at BFs corresponding to the formant frequencies are not seen [12.133]. The nature of the representation used in the cortex is unknown; it is clearly based on a tonotopic axis, but neurons' responses are not determined in a straightforward way by the amount of energy in their tuning curves, as is observed in lower auditory nuclei [12.134]. In some cases, neurons specialized for particular auditory tasks have been found; neurons in one region of the marmoset cortex are tuned to pitch, for example [12.135]. Perhaps the best-studied cases are neurons that respond specifically to species-specific vocalizations in marmosets [12.136] and songbirds [12.137, 138].

## 12.4 Summary

Research on the auditory system has defined the means by which the system efficiently captures sound and couples it into the cochlea, how the frequency analysis of the cochlea is conducted, how transduction occurs, how nonlinear mechanisms involving the OHCs sharpen the frequency tuning, increase the sensitivity, and compress the stimulus intensity, and how suppression acting at the level of AN fibers main-

tains the sharpness of the frequency analysis for complex, multicomponent stimuli. Over the next decade, research on the auditory system will increasingly be focused on the organization and function of the central auditory system, with particular reference to the way in which central neurons derive information from the spectrotemporal display received from the AN.



## References

- 12.1 G.A. Manley, A.N. Popper, R.R. Fay: *Evolution of the Vertebrate Auditory System* (Springer, Berlin, New York 2004)
- 12.2 J.J. Rosowski: Outer and middle ears. In: *Comparative Hearing: Mammals*, ed. by R.R. Fay, A.N. Popper (Springer, Berlin, New York 1994)
- 12.3 J.J. Rosowski: External- and middle-ear function. In: *Auditory Computation*, ed. by H.L. Hawkins, T.A. McMullen, A.N. Popper, R.R. Fay (Springer, Berlin, New York 1996)
- 12.4 E.A.G. Shaw: Transformation of sound pressure level from the free field to the eardrum in the horizontal plane, *J. Acoust. Soc. Am.* **56**, 1848–1861 (1974)
- 12.5 F.M. Wiener, R.R. Pfeiffer, A.S.N. Backus: On the sound pressure transformation by the head and auditory meatus of the cat, *Acta Otolaryngol.* **61**, 255–269 (1966)
- 12.6 J.J. Rice, B.J. May, G.A. Spiron, E.D. Young: Pinna-based spectral cues for sound localization in cat, *Hearing Res.* **58**, 132–152 (1992)
- 12.7 E.A.G. Shaw: External ear response and sound localization. In: *Localization of Sound: Theory and Applications*, ed. by R.W. Gatehouse (Amphora, Groton 1982)
- 12.8 M. Brodel: *Three Unpublished Drawings of the Anatomy of the Human Ear* (Saunders, Philadelphia 1946)
- 12.9 E.A.G. Shaw: 1979 Rayleigh medal lecture: The elusive connection. In: *Localization of Sound: Theory and Applications*, ed. by R.W. Gatehouse (Amphora, Groton 1982)
- 12.10 J.J. Rosowski, L.H. Carney, W.T. Peake: The radiation impedance of the external ear of cat: measurements and applications, *J. Acoust. Soc. Am.* **84**, 1695–1708 (1988)
- 12.11 J.C. Middlebrooks, D.M. Green: Sound localization by human listeners, *Annu. Rev. Psychol.* **42**, 135–159 (1991)
- 12.12 B.J. May, A.Y. Huang: Sound orientation behavior in cats. I. Localization of broadband noise, *J. Acoust. Soc. Am.* **100**, 1059–1069 (1996)
- 12.13 J. Blauert: *Spatial Hearing: The Psychophysics of Human Sound Localization* (MIT Press, Cambridge 1997)
- 12.14 G.F. Kuhn: Physical acoustics and measurements pertaining to directional hearing. In: *Directional Hearing*, ed. by W.A. Yost, G. Gourevitch (Springer, Berlin, New York 1987)
- 12.15 E.D. Young, J.J. Rice, S.C. Tong: Effects of pinna position on head-related transfer functions in the cat, *J. Acoust. Soc. Am.* **99**, 3064–3076 (1996)
- 12.16 A.D. Musicant, J.C.K. Chan, J.E. Hind: Direction-dependent spectral properties of cat external ear: New data and cross-species comparisons, *J. Acoust. Soc. Am.* **87**, 757–781 (1990)
- 12.17 A.Y. Huang, B.J. May: Spectral cues for sound localization in cats: Effects of frequency domain on minimum audible angles in the median and horizontal planes, *J. Acoust. Soc. Am.* **100**, 2341–2348 (1996)
- 12.18 P. Dallos: *The Auditory Periphery, Biophysics and Physiology* (Academic, New York 1973)
- 12.19 J. Zwislocki: Analysis of some auditory characteristics. In: *Handbook of Mathematical Psychology*, ed. by R.D. Luce, R.R. Bush, E. Galanter (Wiley, New York 1965)
- 12.20 W. Bialek: Physical limits to sensation and perception, *Ann. Rev. Biophys. Biophys. Chem.* **16**, 455–478 (1987)
- 12.21 M.B. Sachs, P.J. Abbas: Rate versus level functions for auditory-nerve fibers in cats: tone-burst stimuli, *J. Acoust. Soc. Am.* **56**, 1835–1847 (1974)
- 12.22 P. Wangemann, J. Schacht: Homeostatic mechanisms in the cochlea. In: *The Cochlea*, ed. by P. Dallos, A.N. Popper, R.R. Fay (Springer, Berlin, New York 1996)
- 12.23 W. Bloom, D.W. Fawcett: *A Textbook of Histology* (Saunders, Philadelphia 1975)
- 12.24 D.K. Ryugo: The auditory nerve: Peripheral innervation, cell body morphology, and central projections. In: *The Mammalian Auditory Pathway: Neuroanatomy*, ed. by D.B. Webster, A.N. Popper, R.R. Fay (Springer, Berlin, New York 1992)
- 12.25 W.B. Warr: Organization of olivocochlear efferent systems in mammals. In: *The Mammalian Auditory Pathway: Neuroanatomy*, ed. by D.B. Webster, A.N. Popper, R.R. Fay (Springer, Berlin, New York 1992)
- 12.26 M.C. Brown: Antidromic responses of single units from the spiral ganglion, *J. Neurophysiol.* **71**, 1835–1847 (1994)
- 12.27 D. Robertson: Horseradish peroxidase injection of physiologically characterized afferent and efferent neurons in the guinea pig spiral ganglion, *Hearing Res.* **15**, 113–121 (1984)
- 12.28 D. Robertson, P.M. Sellick, R. Patuzzi: The continuing search for outer hair cell afferents in the guinea pig spiral ganglion, *Hearing Res.* **136**, 151–158 (1999)
- 12.29 D.J. Jagger, G.D. Housley: Membrane properties of type II spiral ganglion neurones identified in a neonatal rat cochlear slice, *J. Physiol.* **552**, 525–533 (2003)
- 12.30 M.A. Reid, J. Flores-Otero, R.L. Davis: Firing patterns of type II spiral ganglion neurons in vitro, *J. Neurosci.* **24**, 733–742 (2004)
- 12.31 J.J. Guinan: Physiology of olivocochlear efferents. In: *The Cochlea*, ed. by P. Dallos, A.N. Popper, R.R. Fay (Springer, Berlin, New York 1996)

- 12.32 M.B. Sachs, I.C. Bruce, E.D. Young: The biological basis of hearing-aid design, *Ann. BME* **30**, 157–168 (2002)
- 12.33 G. von Békésy: *Experiments in Hearing* (McGraw-Hill, New York 1960)
- 12.34 L. Robles, M.A. Ruggero: Mechanics of the mammalian cochlea, *Physiol. Rev.* **81**, 1305–1352 (2001)
- 12.35 D.H. Eldredge: Electrical equivalents of the Békésy traveling wave in the mammalian cochlea. In: *Evoked Electrical Activity in the Auditory Nervous System*, ed. by R.F. Naunton, C. Fernandez (Academic, New York 1978)
- 12.36 M.A. Ruggero, N.C. Rich, A. Recio, S.S. Narayan: Basilar-membrane responses to tones at the base of the chinchilla cochlea, *J. Acoust. Soc. Am.* **101**, 2151–2163 (1997)
- 12.37 N.P. Cooper, W.S. Rhode: Mechanical responses to two-tone distortion products in the apical and basal turns of the mammalian cochlea, *J. Neurophysiol.* **78**, 261–270 (1997)
- 12.38 W.S. Rhode: Observations of the vibration of the basilar membrane in squirrel monkeys using the Mossbauer technique, *J. Acoust. Soc. Am.* **49**, 1218–1231 (1971)
- 12.39 D. Brass, D.T. Kemp: Analyses of Mossbauer mechanical measurements indicate that the cochlea is mechanically active, *J. Acoust. Soc. Am.* **93**, 1502–1515 (1993)
- 12.40 P. Dallos: The active cochlea, *J. Neurosci.* **12**, 4575–4585 (1992)
- 12.41 H. Davis: An active process in cochlear mechanics, *Hear Res.* **9**, 79–90 (1983)
- 12.42 R.J. Diependaal, E. de Boer, M.A. Viergever: Cochlear power flux as an indicator of mechanical activity, *J. Acoust. Soc. Am.* **82**, 917–926 (1987)
- 12.43 G.A. Manley: Evidence for an active process and a cochlear amplifier in nonmammals, *J. Neurophysiol.* **86**, 541–549 (2001)
- 12.44 E. Zwicker: A model describing nonlinearities in hearing by active processes with saturation at 40 dB, *Biol. Cybern.* **35**, 243–250 (1979)
- 12.45 D.T. Kemp: Stimulated acoustic emissions from within the human auditory system, *J. Acoust. Soc. Am.* **64**, 1386–1391 (1978)
- 12.46 C.A. Shera: Mechanisms of mammalian otoacoustic emission and their implications for the clinical utility of otoacoustic emissions, *Ear Hearing* **25**, 86–97 (2004)
- 12.47 C.L. Talmadge, A. Tubis, G.R. Long, C. Tong: Modeling the combined effects of basilar membrane nonlinearity and roughness on stimulus frequency otoacoustic emission fine structure, *J. Acoust. Soc. Am.* **108**, 2911–2932 (2000)
- 12.48 G. Zweig, C.A. Shera: The origin of periodicity in the spectrum of evoked otoacoustic emissions, *J. Acoust. Soc. Am.* **98**, 2018–2047 (1995)
- 12.49 R. Patuzzi: Cochlear micromechanics and macro-mechanics. In: *The Cochlea*, ed. by P. Dallos, A.N. Popper, R.R. Fay (Springer, Berlin, New York 1996)
- 12.50 E. de Boer, A.L. Nuttall, N. Hu, Y. Zou, J. Zheng: The Allen-Fahey experiment extended, *J. Acoust. Soc. Am.* **117**, 1260–1266 (2005)
- 12.51 M.C. Liberman, L.W. Dodds: Single-neuron labeling and chronic cochlear pathology. III. Stereocilia damage and alterations of threshold tuning curves, *Hearing Res.* **16**, 55–74 (1984)
- 12.52 E. Murugasu, I.J. Russell: The effect of efferent stimulation on basilar membrane displacement in the basal turn of the guinea pig cochlea, *J. Neurosci.* **16**, 325–332 (1996)
- 12.53 M.C. Brown, A.L. Nuttall: Efferent control of cochlear inner hair cell responses in the guinea-pig, *J. Physiol.* **354**, 625–646 (1984)
- 12.54 M.L. Wiederhold, N.Y.S. Kiang: Effects of electric stimulation of the crossed olivocochlear bundle on single auditory-nerve fibers in the cat, *J. Acoust. Soc. Am.* **48**, 950–965 (1970)
- 12.55 M.C. Liberman, S. Puria, J.J. Guinan: The ipsilaterally evoked olivocochlear reflex causes rapid adaptation of the  $2f_1-f_2$  distortion product otoacoustic emission, *J. Acoust. Soc. Am.* **99**, 3572–3584 (1996)
- 12.56 D.C. Mountain: Changes in endolymphatic potential and crossed olivocochlear bundle stimulation alter cochlear mechanics, *Science* **210**, 71–72 (1980)
- 12.57 M.A. Ruggero, N.C. Rich, A. Recio: The effect of intense acoustic stimulation on basilar-membrane vibrations, *Aud. Neurosci.* **2**, 329–345 (1996)
- 12.58 A.J. Oxenham, S.P. Bacon: Cochlear compression: Perceptual measures and implications for normal and impaired hearing, *Ear Hearing* **24**, 352–366 (2003)
- 12.59 D.A. Nelson, A.C. Schroder, M. Wojtczak: A new procedure for measuring peripheral compression in normal-hearing and hearing-impaired listeners, *J. Acoust. Soc. Am.* **110**, 2045–2064 (2001)
- 12.60 A.J. Oxenham, C.J. Plack: A behavioral measure of basilar-membrane nonlinearity in listeners with normal and impaired hearing, *J. Acoust. Soc. Am.* **101**, 3666–3675 (1997)
- 12.61 E. de Boer: Mechanics of the cochlea: Modeling efforts. In: *The Cochlea*, ed. by P. Dallos, A.N. Popper, R.R. Fay (Springer, Berlin, New York 1996)
- 12.62 A.E. Hubbard, D.C. Mountain: Analysis and synthesis of cochlear mechanical function using models. In: *Auditory Computation*, ed. by H.L. Hawkins, T.A. McMullen, A.N. Popper, R.R. Fay (Springer, Berlin, New York 1996)
- 12.63 R.C. Naidu, D.C. Mountain: Measurements of the stiffness map challenge a basic tenet of cochlear theories, *Hearing Res.* **124**, 124–131 (1998)
- 12.64 M.P. Sherer, A.W. Gummer: Impedance analysis of the organ of corti with magnetically actuated probes, *Biophys. J.* **87**, 1378–1391 (2004)

- 12.65 M.B. Sachs: Speech encoding in the auditory nerve. In: *Hearing Science Recent Advances*, ed. by C.I. Berlin (College Hill, San Diego 1984)
- 12.66 J.J. Eggermont: Between sound and perception: reviewing the search for a neural code, *Hear Res.* **157**, 1–42 (2001)
- 12.67 B.C.J. Moore: Coding of sounds in the auditory system and its relevance to signal processing and coding in cochlear implants, *Otol. Neurotol.* **24**, 243–254 (2003)
- 12.68 I.C. Bruce, M.B. Sachs, E.D. Young: An auditory-periphery model of the effects of acoustic trauma on auditory nerve responses, *J. Acoust. Soc. Am.* **113**, 369–388 (2003)
- 12.69 S.D. Holmes, C. Sumner, L.P. O'Mard, R. Meddis: The temporal representation of speech in a nonlinear model of the guinea pig cochlea, *J. Acoust. Soc. Am.* **116**, 3534–3545 (2004)
- 12.70 X. Zhang, M.G. Heinz, I.C. Bruce, L.H. Carney: A phenomenological model for the responses of auditory-nerve fibers: I. Nonlinear tuning with compression and suppression, *J. Acoust. Soc. Am.* **109**, 648–670 (2001)
- 12.71 H.S. Colburn, L.H. Carney, M.G. Heinz: Quantifying the information in auditory-nerve responses for level discrimination, *J. Assoc. Res. Otolaryngol.* **4**, 294–311 (2003)
- 12.72 B.C.J. Moore: *An Introduction to the Psychology of Hearing* (Elsevier, London 2004)
- 12.73 P.A. Cariani, B. Delgutte: Neural correlates of the pitch of complex tones. II. Pitch shift, pitch ambiguity, phase invariance, pitch circularity, rate pitch, and the dominance region for pitch, *J. Neurophysiol.* **76**, 1717–1734 (1996)
- 12.74 R.L. Miller, J.R. Schilling, K.R. Franck, E.D. Young: Effects of acoustic trauma on the representation of the vowel /e/ in cat auditory nerve fibers, *J. Acoust. Soc. Am.* **101**, 3602–3616 (1997)
- 12.75 D.H. Johnson: The relationship of post-stimulus time and interval histograms to the timing characteristics of spike trains, *Biophys. J.* **22**(3), 413–430 (1978)
- 12.76 M.C. Liberman: Auditory-nerve response from cats raised in a low-noise chamber, *J. Acoust. Soc. Am.* **63**, 442–455 (1978)
- 12.77 G.K. Yates, I.M. Winter, D. Robertson: Basilar membrane nonlinearity determines auditory nerve rate-intensity functions and cochlear dynamic range, *Hearing Res.* **45**, 203–220 (1990)
- 12.78 B.C.J. Moore: *Perceptual Consequences of Cochlear Damage* (Oxford Univ. Press, Oxford 1995)
- 12.79 M.G. Heinz, J.B. Issa, E.D. Young: Auditory-nerve rate responses are inconsistent with common hypotheses for the neural correlates of loudness recruitment, *J. Assoc. Res. Otolaryngol.* **6**, 91–105 (2005)
- 12.80 J.O. Pickles: Auditory-nerve correlates of loudness summation with stimulus bandwidth, in normal and pathological cochleae, *Hearing Res.* **12**, 239–250 (1983)
- 12.81 E.M. Relkin, J.R. Doucet: Is loudness simply proportional to the auditory nerve spike count?, *J. Acoust. Soc. Am.* **101**, 2735–2740 (1997)
- 12.82 S. Rosen: Temporal information in speech: acoustic, auditory and linguistic aspects, *Philos. Trans. R. Soc. London B.* **336**, 367–373 (1992)
- 12.83 A.R. Palmer, I.J. Russell: Phase-locking in the cochlear nerve of the guinea-pig and its relation to the receptor potential of inner hair-cells, *Hear Res.* **24**, 1–15 (1986)
- 12.84 T.C.T. Yin: Neural mechanisms of encoding binaural localization cues in the auditory brainstem. In: *Integrative Functions in the Mammalian Auditory Pathway*, ed. by D. Oertel, A.N. Popper, R.R. Fay (Springer, Berlin, New York 2002)
- 12.85 S.A. Shamma: Speech processing in the auditory system. II: Lateral inhibition and the central processing of speech evoked activity in the auditory nerve, *J. Acoust. Soc. Am.* **78**, 1622–1632 (1985)
- 12.86 P. Dallos, B. Fakler: Prestin, a new type of motor protein, *Nature Rev. Molec. Bio.* **3**, 104–111 (2002)
- 12.87 R.A. Eatock, K.M. Hurley: Functional development of hair cells, *Curr. Top. Dev. Bio.* **57**, 389–448 (2003)
- 12.88 R. Fettiplace, C.M. Hackney: The sensory and motor roles of auditory hair cells, *Nature Rev. Neurosci.* **7**, 19–29 (2006)
- 12.89 M. LeMasurier, P.G. Gillespie: Hair-cell mechanotransduction and cochlear amplification, *Neuron.* **48**, 403–415 (2005)
- 12.90 G.I. Frolenkov, I.A. Belyantseva, T.B. Friedmann, A.J. Griffith: Genetic insights into the morphogenesis of inner ear hair cells, *Nature Rev. Genet.* **5**, 489–498 (2004)
- 12.91 J.O. Pickles, S.D. Comis, M.P. Osborne: Cross-links between stereocilia in the guinea pig organ of Corti, and their possible relation to sensory transduction, *Hear Res.* **15**, 103–112 (1984)
- 12.92 A. Flock: Transducing mechanisms in the lateral line canal organ receptors, *Cold Spring Harb. Symp. Quant. Biol.* **30**, 133–145 (1965)
- 12.93 S.L. Shotwell, R. Jacobs, A.J. Hudspeth: Directional sensitivity of individual vertebrate hair cells to controlled deflection of their hair bundles, *Ann. NY Acad. Sci.* **374**, 1–10 (1981)
- 12.94 J.A. Assad, G.M.G. Shepherd, D.P. Corey: Tip-link integrity and mechanical transduction in vertebrate hair cells, *Neuron* **7**, 985–994 (1991)
- 12.95 M.A. Ruggero, N.C. Rich: Timing of spike initiation in cochlear afferents: dependence on site of innervation, *J. Neurophysiol.* **58**, 379–403 (1987)
- 12.96 E. Glowatzki, P.A. Fuchs: Transmitter release at the hair cell ribbon synapse, *Nature Neurosci.* **5**, 147–154 (2002)
- 12.97 L.O. Trussell: Transmission at the hair cell synapse, *Nature Neurosci.* **5**, 85–86 (2002)

- 12.98 Y. Raphael, R.A. Altschuler: Structure and innervation of the cochlea, *Brain Res. Bull.* **60**, 397–422 (2003)
- 12.99 P.G. Gillespie, J.L. Cyr: Myosin-1c, the hair cell's adaptation motor, *Annu. Rev. Physiol.* **66**, 521–545 (2004)
- 12.100 M.C. Holley: Outer hair cell motility. In: *The Cochlea*, ed. by P. Dallos, A.N. Popper, R.R. Fay (Springer, Berlin, New York 1996)
- 12.101 R. Fettiplace: Active hair bundle movements in auditory hair cells, *J. Physiol.* **576**, 29–36 (2006)
- 12.102 M.C. Brown, A.L. Nuttall, R.I. Masta: Intracellular recordings from cochlear inner hair cells: effects of stimulation of the crossed olivocochlear efferents, *Science* **222**, 69–72 (1983)
- 12.103 D.F. Dolan, M.H. Guo, A.L. Nuttall: Frequency-dependent enhancement of basilar membrane velocity during olivocochlear bundle stimulation, *J. Acoust. Soc. Am.* **102**, 3587–3596 (1997)
- 12.104 J. Santos-Sacchi: Reversible inhibition of voltage-dependent outer hair cell motility and capacitance, *J. Neurosci.* **11**, 3096–3110 (1991)
- 12.105 P. Dallos, D. Harris: Properties of auditory nerve responses in absence of outer hair cells, *J. Neurophysiol.* **41**, 365–383 (1978)
- 12.106 M.C. Liberman, N.Y. Kiang: Single-neuron labeling and chronic cochlear pathology. IV. Stereocilia damage and alterations in rate- and phase-level functions, *Hearing Res.* **16**, 75–90 (1984)
- 12.107 J.F. Ashmore: A fast motile response in guinea pig outer hair cells: the basis of the cochlear amplifier, *J. Physiol.* **388**, 323–347 (1987)
- 12.108 W.E. Brownell, C.R. Bader, D. Bertrand, Y. de Ribaupierre: Evoked mechanical responses of isolated cochlear hair cells, *Science* **227**, 194–196 (1985)
- 12.109 I.A. Belyantseva, H.J. Adler, R. Curi, G.I. Frolenkov, B. Kachar: Expression and localization of prestin and the sugar transporter GLUT-5 during development of electromotility in cochlear outer hair cell, *J. Neurosci.* **20**(RC116), 1–5 (2000)
- 12.110 F. Kalinec, M.C. Holley, K.H. Iwasa, D.J. Lim, B. Kachar: A membrane-based force generation mechanism in auditory sensory cells, *Proc. Natl. Acad. Sci. USA* **89**, 8671–8675 (1992)
- 12.111 J. Zheng, W. Shen, D.Z. He, K.B. Long, D. Madison, P. Dallos: Prestin is the motor protein of cochlear outer hair cells, *Nature* **405**, 149–155 (2000)
- 12.112 M.C. Holley, F. Kalinec, B. Kachar: Structure of the cortical cytoskeleton in mammalian outer hair cells, *J. Cell Sci.* **102**, 569–580 (1992)
- 12.113 D. Oliver, D.Z. He, N. Klocker, J. Ludwig, U. Schutte, S. Waldegger, J.P. Ruppersberg, P. Dallos, B. Fakler: Intracellular anions as the voltage sensor of prestin, the outer hair cell motor protein, *Science* **292**, 2340–2343 (2001)
- 12.114 M.C. Liberman, J. Galilo, D.Z.Z. He, X. Wu, S. Jia, J. Zuo: Prestin is required for electromotility of the outer hair cell and for the cochlear amplifier, *Nature* **419**, 300–304 (2002)
- 12.115 C.D. Geisler, C. Sang: A cochlear model using feed-forward outer-hair-cell forces, *Hear Res.* **86**, 132–146 (1995)
- 12.116 P.A. Fuchs: Synaptic transmission at vertebrate hair cells, *Curr. Opin. Neurobiol.* **6**, 514–519 (1996)
- 12.117 D.O. Kim, C.E. Molnar, J.W. Matthews: Cochlear mechanics: Nonlinear behavior in two-tone responses as reflected in cochlear-nerve-fiber responses and in ear-canal sound pressure, *J. Acoust. Soc. Am.* **67**, 1704–1721 (1980)
- 12.118 E. Javel, C.D. Geisler, A. Ravindran: Two-tone suppression in auditory nerve of the cat: rate-intensity and temporal analyses, *J. Acoust. Soc. Am.* **63**(4), 1093–1104 (1978)
- 12.119 M.B. Sachs, N.Y. Kiang: Two-tone inhibition in auditory-nerve fibers, *J. Acoust. Soc. Am.* **43**(5), 1120–1128 (1968)
- 12.120 E.D. Young, M.B. Sachs: Representation of steady-state vowels in the temporal aspects of the discharge patterns of populations of auditory-nerve fibers, *J. Acoust. Soc. Am.* **66**, 1381–1403 (1979)
- 12.121 M.B. Sachs, E.D. Young: Encoding of steady-state vowels in the auditory nerve: Representation in terms of discharge rate, *J. Acoust. Soc. Am.* **66**, 470–479 (1979)
- 12.122 J.C. Wong, R.L. Miller, B.M. Callhoun, M.B. Sachs, E.D. Young: Effects of high sound levels on responses to the vowel /e/ in cat auditory nerve, *Hear Res.* **123**, 61–77 (1998)
- 12.123 G. Ehret, R. Romand: *The Central Auditory System* (Oxford Univ. Press, New York 1997)
- 12.124 M.S. Malmierca, D.R.F. Irvine: *International Review of Neurobiology – Auditory Spectral Processing*, Vol. 70 (Elsevier, Amsterdam 2005)
- 12.125 D. Oertel, A.N. Popper, R.R. Fay: *Integrative Functions in the Mammalian Auditory Pathway* (Springer, Berlin, New York 2001)
- 12.126 J.A. Winer, C.E. Schreiner: *The Inferior Colliculus* (Springer, Berlin, New York 2005)
- 12.127 S.P. Bacon, A.J. Oxenham: Psychophysical manifestations of compression: Hearing-impaired listeners. In: *Compression: From cochlea to cochlear implants*, ed. by S.P. Bacon, R.R. Fay, A.N. Popper (Springer, Berlin, New York 2004)
- 12.128 C.C. Blackburn, M.B. Sachs: The representations of the steady-state vowel sound /e/ in the discharge patterns of cat anteroventral cochlear nucleus neurons, *J. Neurophysiol.* **63**, 1191–1212 (1990)
- 12.129 A.R. Palmer: Reassessing mechanisms of low-frequency sound localisation, *Curr. Opin. Neurobiol.* **14**, 457–460 (2004)
- 12.130 A.R. Palmer, D. Jiang, D. McAlpine: Neural responses in the inferior colliculus to binaural masking level differences created by inverting the

- noise in one ear, *J. Neurophysiol.* **84**, 844–852 (2000)
- 12.131 T.C. Yin: Physiological correlates of the precedence effect and summing localization in the inferior colliculus of the cat, *J. Neurosci.* **14**, 5170–5186 (1994)
- 12.132 I. Nelken: Processing of complex stimuli and natural scenes in the auditory cortex, *Curr. Opin. Neurobiol.* **14**, 474–480 (2004)
- 12.133 S.W. Wong, C.E. Schreiner: Representation of CV-sounds in cat primary auditory cortex: Intensity dependence, *Speech Commun.* **41**, 93–106 (2003)
- 12.134 C.K. Machens, M.S. Wehr, A.M. Zador: Linearity of cortical receptive fields measured with natural sounds, *J. Neurosci.* **24**, 1089–1100 (2004)
- 12.135 D. Bendor, X. Wang: The neuronal representation of pitch in primate auditory cortex, *Nature* **436**, 1161–1165 (2005)
- 12.136 X. Wang, S.C. Kadia: Differential representation of species-specific primate vocalizations in the auditory cortices of marmoset and cat, *J. Neurophysiol.* **86**, 2616–2620 (2001)
- 12.137 H. Cousillas, H.J. Leppelsack, E. Leppelsack, J.P. Richard, M. Mathelier, M. Hausberger: Functional organization of the forebrain auditory centres of the European starling: A study based on natural sounds, *Hear Res.* **207**, 10–21 (2005)
- 12.138 J.A. Grace, N. Amin, N.C. Singh, F.E. Theunissen: Selectivity for conspecific song in the zebra finch auditory forebrain, *J. Neurophysiol.* **89**, 472–487 (2003)